

Organic Geochemistry

Carbon and sulfur isotopic composition of alkyl- and benzo-thiophenes provides insights to their origin and formation pathways

--Manuscript Draft--

Manuscript Number:	
Article Type:	Research Paper
Keywords:	Benzothiophenes, Alkylthiophenes, Organic S compounds, Compound specific S and C isotopes, Biomarkers, Ghareb Formation
Corresponding Author:	Alon Amrani, PhD Hebrew University of Jerusalem Jerusalem, ISRAEL
First Author:	Lubna Shawar
Order of Authors:	Lubna Shawar Kliti Grice Alex Holman Alon Amrani, PhD
Abstract:	<p>Thiophenic compounds can provide significant geochemical information and may be used as paleoenvironmental indicators as long as their biological origin and formation pathways are understood. To this end, we investigated the structures, distribution, $\delta^{13}\text{C}$ and $\delta^{34}\text{S}$ values of specific thiophenic compounds extracted from immature sedimentary rocks from the Upper Cretaceous (Ghareb Formation, Shefela Basin, Israel).</p> <p>Isoprenoidal alkylthiophenes (ATs) show a general trend of depletion in their ^{13}C and ^{34}S relative to the normal (linear) ATs extracted from the studied samples. In addition, a consistent enrichment of up to 2‰ in ^{13}C and 8‰ in ^{34}S of methylated ATs ($m/z=111$) relative to non-methylated ones ($m/z=97$) was recorded. This suggests that AT precursors derived from different organisms and diagenetic pathways which later affected their sulfurization mechanisms. The large variation in $\delta^{34}\text{S}$ values of individual ATs, ~15 ‰, along with the general trend of ^{13}C depletion with increasing T_{max} suggests that ATs formed by a set of diagenetic processes of mild thermochemical alteration. The $\delta^{13}\text{C}$ values of BTs are enriched in ^{13}C relative to the rest of OSCs, by ~3‰ in average. This in turn suggests that BTs were generated mainly by sulfurization and subsequent ring closure or aromatization of ^{13}C enriched aromatic/ alkyl cyclohexane compounds with unsaturation and/or functional groups in their alkyl chain. Such ^{13}C enriched precursors can be generated from carotenoids and terrestrial compounds (e.g., by lignin degradation). The large variation in $\delta^{34}\text{S}$ values of individual BTs, ~15 ‰, suggests that the BTs in our samples are formed during the diagenesis stage and did not experience advanced thermal alteration processes. Therefore, their occurrence in immature sedimentary rocks might be used as a proxy for early thermochemical alterations that cannot be detected using conventional geochemical indicators, such as T_{max}.</p> <p>The combination of structural, ^{13}C and ^{34}S investigation of individual OSCs enhanced our understanding of their sulfurization pathways and origin which in turn will help develop new paleoenvironmental indicators.</p>

Highlights



- Thiophenic compounds (benzothiophenes and alkylthiophenes) show unique ^{13}C and ^{34}S trends in the immature Ghareb Formation rocks.
- Benzothiophenes originated from ^{13}C enriched compounds such as carotenoids and terrestrial material.
- The presence of appropriate functionalized precursors and inorganic (poly)sulfides are essential for low temperature thiophenic compound formation.
- Thiophenic compounds formed as a result of multiple diagenetic sulfurization pathways followed by mild thermochemical alterations.
- Thiophenic compound distributions, and their associated S and C isotope composition can be used as a proxy for diagenetic thermochemical alteration.

1
2
3
4 **1 Carbon and sulfur isotopic composition of alkyl- and benzo-thiophenes provides**
5
6 **2 insights to their origin and formation pathways**
7
8

9
10 3 Lubna Shawar ^a, Kliti Grice ^b, Alex I. Holman ^b and Alon Amrani ^a
11

12 4 ^a Institute of Earth Sciences, Hebrew University, Jerusalem, Israel
13
14

15
16 5 ^b WA Organic & Isotope Geochemistry Centre, The Institute for Geoscience Research,
17
18 6 School of Earth and Planetary Sciences, Curtin University, Australia
19
20

21 7 *Corresponding author: Alon.Amrani@mail.huji.ac.il
22
23

24
25 8 **Highlights**
26

- 27
28 9 • Thiophenic compounds (benzothiophenes and alkylthiophenes) show unique ¹³C
29
30 10 and ³⁴S trends in the immature Ghareb Formation rocks.
31
32
33 11 • Benzothiophenes originated from ¹³C enriched compounds such as carotenoids and
34
35 12 terrestrial material.
36
37
38 13 • The presence of appropriate functionalized precursors and inorganic (poly)sulfides
39
40 14 are essential for low temperature thiophenic compound formation.
41
42
43 15 • Thiophenic compounds formed as a result of multiple diagenetic sulfurization
44
45 16 pathways followed by mild thermochemical alterations.
46
47
48 17 • Thiophenic compound distributions, and their associated S and C isotope
49
50 18 composition can be used as a proxy for diagenetic thermochemical alteration.
51
52

53 19 **Abstract**
54

55
56 20 Thiophenic compounds can provide significant geochemical information and may be used
57
58 21 as paleoenvironmental indicators as long as their biological origin and formation pathways
59
60
61
62
63
64
65

1
2
3
4 22 are understood. To this end, we investigated the structures, distribution, $\delta^{13}\text{C}$ and $\delta^{34}\text{S}$
5
6
7 23 values of specific thiophenic compounds extracted from immature sedimentary rocks from
8
9 24 the Upper Cretaceous (Ghareb Formation, Shefela Basin, Israel).

10
11
12 25 Isoprenoidal alkylthiophenes (ATs) show a general trend of depletion in their ^{13}C and ^{34}S
13
14
15 26 relative to the normal (linear) ATs extracted from the studied samples. In addition, a
16
17 27 consistent enrichment of up to 2‰ in ^{13}C and 8‰ in ^{34}S of methylated ATs ($m/z= 111$)
18
19 28 relative to non-methylated ones ($m/z= 97$) was recorded. This suggests that AT precursors
20
21
22 29 derived from different organisms and diagenetic pathways which later affected their
23
24
25 30 sulfurization mechanisms. The large variation in $\delta^{34}\text{S}$ values of individual ATs, ~15 ‰,
26
27 31 along with the general trend of ^{13}C depletion with increasing T_{max} suggests that ATs formed
28
29
30 32 by a set of diagenetic processes of mild thermochemical alteration. The $\delta^{13}\text{C}$ values of BTs
31
32
33 33 are enriched in ^{13}C relative to the rest of OSCs, by ~3‰ in average. This in turn suggests
34
35 34 that BTs were generated *mainly* by sulfurization and subsequent ring closure or
36
37 35 aromatization of ^{13}C enriched aromatic/ alkyl cyclohexane compounds with unsaturation
38
39 36 and/or functional groups in their alkyl chain. Such ^{13}C enriched precursors can be generated
40
41
42 37 from carotenoids and terrestrial compounds (e.g., by lignin degradation). The large
43
44 38 variation in $\delta^{34}\text{S}$ values of individual BTs, ~15 ‰, suggests that the BTs in our samples
45
46
47 39 are formed during the diagenesis stage and did not experience advanced thermal alteration
48
49
50 40 processes. Therefore, their occurrence in immature sedimentary rocks might be used as a
51
52 41 proxy for early thermochemical alterations that cannot be detected using conventional
53
54 42 geochemical indicators, such as T_{max} .
55
56
57
58
59
60
61
62
63
64
65

1
2
3
4 43 The combination of structural, ^{13}C and ^{34}S investigation of individual OSCs enhanced our
5
6
7 44 understanding of their sulfurization pathways and origin which in turn will help develop
8
9 45 new paleoenvironmental indicators.

10 11 12 46 **Keywords**

13
14
15 47 Benzothiophenes, Alkylthiophenes, Organic S compounds, Compound specific S and C
16
17
18 48 isotopes, Biomarkers, Ghareb Formation

19 20 21 49 **1. Introduction**

22
23
24 50 Organic sulfur compounds (OSCs) are generated during early diagenesis and linked to local
25
26
27 51 and global paleo-environmental events ([Sinninghe Damste and de Leeuw, 1990](#); [Werne et](#)
28
29 52 [al., 2004](#); [Kutuzov et al., 2019](#)). OSCs found in sedimentary rocks often resemble their
30
31
32 53 biomolecular precursors and thus they can serve as biomarkers ([Brassel et al., 1986](#);
33
34 54 [Schaeffer et al., 1995](#); [Grice et al., 1998](#)). They form as a result of reduced sulfur (e.g. HS^-
35
36 55 , S_x^{2-}) incorporation into functionalized sites of biomolecules and this in turn enhances the
37
38
39 56 preservation of their carbon skeleton by binding them to macromolecular fractions
40
41
42 57 ([Aizenshtat et al., 1983](#); [Kohnen et al., 1989](#); [Adam et al., 1993](#); [Amrani, 2014](#)). Moreover,
43
44 58 saturation of double bonds with H_2S was suggested as a geochemical pathway that
45
46 59 enhances the preservation of poly-unsaturated biomarkers such as carotenoids ([Hebting et](#)
47
48 60 [al., 2006](#)).

50
51
52 61 Reduced S species, in anoxic environments, are generated by dissimilatory microbial
53
54 62 sulfate reduction (MSR) ([Kaplan et al., 1963](#)). This process occurs at low temperatures (<
55
56 63 80°C) and it is associated with large S isotope fractionation (up to $\sim 75\%$) ([Wortmann et](#)
57
58 64 [al., 2001](#); [Brunner and Bernasconi, 2005](#); [Canfield et al., 2010](#); [Sim et al., 2011](#)). The S

1
2
3
4 65 isotope fractionation associated with MSR processes is recorded in the isotopic
5
6 66 composition of organic and inorganic S species (e.g. pyrite) in sediments and sedimentary
7
8
9 67 rocks ([Anderson and Pratt, 1995](#); [Canfield et al., 1998](#); [2010](#); [Amrani, 2014](#)).

10
11
12 68 Alkylthiophenes (ATs) and fused thiophenes (e.g., benzothiophenes (BTs)) are abundant
13
14 69 sub-groups of OSCs ([Sinninghe Damste and de Leeuw, 1990](#); [Kutuzov et al., 2019](#)). Many
15
16
17 70 ATs, such as iC₂₀ thiophenes, were detected in recent sediments, in mature and immature
18
19 71 organic rich rocks, oils and natural gas ([Brassell et al., 1986](#); [de Leeuw and Sinninghe](#)
20
21
22 72 [Damsté, 1990](#); [Barakat and Rullkötter, 1995](#); [Adam et al., 2000](#); [Russell et al., 2000](#)). The
23
24 73 relative abundances of ATs and their isomers allow qualitative interpretations such as the
25
26
27 74 environmental conditions involved during OM deposition. For instance, under hypersaline
28
29 75 conditions, archaeal populations that produce polyunsaturated phytenols are favored.
30
31
32 76 Sulfurization of these compounds yields isoprenoidal mid-chain thiophenes ([Sinninghe](#)
33
34 77 [Damsté et al., 1989b](#); [Kohnen et al., 1990b](#); [Barakat and Rullkötter, 1995](#); [Schwark et al.,](#)
35
36 78 [1998](#)). Thus, the distribution of i-C₂₀ thiophene (phytol thiophene) isomers is proposed as
37
38
39 79 a proxy for paleo-salinity ([Sinninghe Damsté et al., 1989b](#); [de Leeuw and Sinninghe](#)
40
41 80 [Damsté, 1990](#); [Barakat and Rullkötter, 1995](#)). Studies that investigated the $\delta^{13}\text{C}$ values of
42
43
44 81 ATs have shown that a certain carbon skeleton of AT can have multiple biosynthetic
45
46 82 precursors which are, in a number of cases, derived from several biological sources
47
48
49 83 ([Kohnen et al., 1992a](#); [1992b](#)). Therefore, ATs product-precursor relation to study origin
50
51
52 84 and formation process is sometimes limited. Recent studies have investigated $\delta^{34}\text{S}$ values
53
54 85 of ATs, alongside another OSCs, in order to learn their formation process and the paleo-
55
56 86 environmental conditions involved in their formation ([Raven et al., 2015](#); [2016](#); [Shawar et](#)
57
58
59 87 [al., 2020](#)). [Raven et al. \(2015\)](#) studied recent sediments from the Cariaco Basin. They

1
2
3
4
5
6
7
8
9
10
11
12
13
14
15
16
17
18
19
20
21
22
23
24
25
26
27
28
29
30
31
32
33
34
35
36
37
38
39
40
41
42
43
44
45
46
47
48
49
50
51
52
53
54
55
56
57
58
59
60
61
62
63
64
65

88 showed a large variation in $\delta^{34}\text{S}$ values of different OSCs, up to 25‰, with some OSCs
89 (e.g. isoprenoid C₂₀ thiophenes) that are ³⁴S depleted relative to the coexisting pyrite. They
90 suggested that the sulfurization occurred through two different pathways, reversible and
91 irreversible. [Shawar et al. \(2020\)](#) studied the ancient and immature organic-rich rocks from
92 the Cretaceous Ghareb (Shefela Basin, Israel) and Miocene Monterey (Naples Beach,
93 USA) Formations. Large variations in the $\delta^{34}\text{S}$ values of different OSCs, that reached up
94 to 28‰ and 36‰, were observed in the Ghareb and Monterey samples, respectively.
95 Additionally, they showed that $\delta^{34}\text{S}$ values of C₂₅ highly branched isoprenoid thiophene
96 might be used as a proxy for the euxinic sulfurization environment ([Shawar et al., 2020](#)).
97 Benzothiophenes (BTs) usually occur in oils but rarely in immature rocks ([Orr, 1986](#);
98 [Schou and Myhr, 1988](#); [Chakhmakhchev and Suzuki, 1995](#)). They have been mainly used
99 as a proxy for thermal maturation assessment in oils (e.g., [Ho et al., 1974](#); [Orr, 1986](#);
100 [Radke, 1988](#); [Schou and Myhr, 1988](#); [Chakhmakhchev and Suzuki, 1995](#)). Only few
101 studies have used BTs in oils as a proxy for depositional environment (siliceous versus
102 carbonate rich environment; e.g., [Hughes, 1984](#)), most likely because their origin is still
103 debated. Surprisingly, we could not find any study regarding the $\delta^{13}\text{C}$ values of BTs in the
104 scientific literature. Sulfur isotope studies had used them as tracers for thermochemical
105 sulfate reduction (TSR) as well as proxies for oil-oil and oil-source rock correlations
106 ([Amrani et al., 2012](#); [Amrani, 2014](#); [Cai et al., 2015](#); [Meshoulam et al., 2016](#); [Greenwood](#)
107 [et al., 2018](#)). However, a recent study has reported that BTs are abundant also in *immature*
108 organic rich sedimentary rocks from the Ghareb Formation, Israel ([Shawar et al., 2020](#)).
109 Moreover, these BTs vary in their $\delta^{34}\text{S}$ values by ~15‰, much larger than the 2‰ variation
110 reported in $\delta^{34}\text{S}$ values of BTs generated during artificial thermal maturation or the <5‰

1
2
3
4 111 variation of natural thermal maturation (non TSR) processes (Ellis et al., 2017; Rosenberg
5
6 112 et al., 2017). The origin and formation pathways of these thermally “immature” BTs are
7
8
9 113 not understood and may have important geochemical implications (Shawar et al., 2020).

10
11
12 114 The recent compound-specific sulfur isotope analysis (CSSIA) studies demonstrated the
13
14
15 115 potential of OSCs as paleoenvironmental tools (Raven et al., 2015;2016; Shawar et al.,
16
17 116 2020). Coupling $\delta^{13}\text{C}$ of individual OSCs to their $\delta^{34}\text{S}$ values may further improve our
18
19
20 117 understanding of their precursors and formation pathways.

21
22 118 In the present study, we investigate the origin of OSCs and their mechanism of formation
23
24
25 119 and attempt to draw possible sulfurization pathways and their associated paleo-
26
27 120 environmental conditions. Immature rock samples from the Late Cretaceous Ghareb
28
29 121 Formation (Shefela Basin, Israel) were used as a test case in continuation of our previous
30
31
32 122 studies of these samples (Shawar et al., 2018; 2020). We applied compound specific C
33
34
35 123 isotope analyses on saturates, biomarkers and OSC on these rock extracts. We then
36
37 124 combined these results with the previously published (Shawar et al., 2020) CSSIA data of
38
39 125 ATs and BTs.

42 126 **2. Methods**

45 127 *2.1 Study sites*

46
47
48 128 Nine core samples of the Late Cretaceous organic-rich chalk sequence were analyzed.
49
50
51 129 These samples were drilled from 260 m to 600 m below the surface in the Ghareb
52
53 130 Formation, Aderet borehole, the depo-center of the Shefela Basin (hereafter Ghareb
54
55 131 Formation). These sediments represent a high-productivity succession developed at the
56
57
58 132 Late Cretaceous outer shelf belt due to an extensive upwelling system along the southern
59
60
61
62
63
64
65

1
2
3
4 133 Tethyan margin (Almogi-Labin et al., 1993; Eshet and Almogi-Labin, 1996; Soudry et al.,
5
6 134 2006; Meilijson et al., 2014). Detailed descriptions of these samples and their lithologies
7
8
9 135 are given by Shavar et al. (2018).

10 11 136 *2.2 Materials and standards*

12
13
14
15 137 Analytical grade solvents used in this study (dichloromethane, hexane, methanol, etc.) were
16
17 138 purchased from Biolab Ltd. (Jerusalem, Israel) and were distilled before use. Sulfur
18
19 139 hexafluoride was purchased from Praxair Inc. (PA, USA). The S isotope reference
20
21 140 materials NBS-127 (BaSO₄; δ³⁴S = 21.1‰), IAEA-S-1 (Ag₂S; δ³⁴S = -0.3‰), and IAEA-
22
23 141 SO-6 (BaSO₄; δ³⁴S = -34.1‰) were purchased from the National Institute of Standards and
24
25
26
27 142 Technology (NIST, USA) and used for calibration of in-house standards. All other
28
29 143 chemicals (>99% purity) were purchased from Sigma-Aldrich (St. Louis, USA).

30 31 32 33 144 *2.3 Organic extraction*

34
35
36 145 Bitumen was extracted from 160 g of powdered rock, with a mixture of organic solvents
37
38 146 (9:1, dichloromethane: methanol, 7 mL/g rock), for each core sample from the Ghareb
39
40 147 Formation. The samples were extracted using a microwave accelerated solvent extractor
41
42 148 (MARS5 Express, CEM Corporation, USA) at 120°C for 30 minutes. The microwave
43
44 149 extraction was repeated twice to ensure complete extraction of the bitumen. Asphaltene
45
46 150 separation from the dried and concentrated bitumen was achieved by dissolution of the
47
48 151 bitumen with *n*-pentane (50:1 bitumen weight) overnight. The maltene fraction was
49
50
51 152 evaporated and weighed. Detailed descriptions of this method are given by Shavar et al.,
52
53
54 153 (2020).

55 56 57 58 59 154 *2.4 Sample preparation for OSC quantification and CSSIA*

60
61
62
63
64
65

1
2
3
4 155 *2.4.1 Liquid chromatography (LC)*

5
6
7 156 About 140 mg of the maltenes were separated by liquid chromatography (LC) into five
8
9 157 sub-fractions (saturated hydrocarbons, alkylthiophenes (ATs), benzothiophenes (BTs),
10
11 158 sulfidic and polar compounds). A detailed description of this method is given by [Shawar](#)
12
13 159 [et al., \(2020\)](#).
14
15
16

17
18 160 *2.4.2 Identification and quantification of OSC (GC-MS, GC-FPD and GC-QQQ-MS*
19
20 161 *analysis)*
21
22

23 162 All details related to the analysis, quantification, and CSSIA of OSCs are published
24
25 163 previously in [Shawar et al., \(2020\)](#).
26
27

28
29 164 For the identification and quantification of biomarkers (such as carotenoid biomarkers
30
31 165 (isorenieratane, β -isorenieratane, β -carotene, γ -carotene, dimethyl/diethyl carotenoids, and
32
33 166 dimethyl diaromatic carotenoids) and perylene) in non-polar fractions (the combination of
34
35 167 saturates, ATs and BTs) a gas chromatograph coupled to triple quadrupole mass
36
37 168 spectrometer (GC-QQQ-MS; Agilent 7890B/7010, USA) was used. 1 μ l of sample was
38
39 169 injected into the device via multi-mode inlet using an auto-sampler. The inlet temperature
40
41 170 was ramped from 60°C to 340°C at a rate of 70°C/min. The injection was carried out in a
42
43 171 splitless mode. The carrier gas was at a constant rate flow of 1.5 mL/min. The GC oven
44
45 172 temperature was programmed at 60°C for 2 min then 8°C/min to 220°C, then 2°C/min to
46
47 173 320°C min and held for 28 min. The transfer line temperature was held at 320°C. The
48
49 174 quadrupole analyzer and the MS source were operated at 150°C and 270°C, respectively,
50
51 175 in electron impact mode at 70 eV. The GC-MS system was equipped with an Agilent DB-
52
53 176 5MS capillary column (60m \times 250 μ m \times 0.25 μ m).
54
55
56
57
58
59
60
61
62
63
64
65

1
2
3
4 177 2.5 *Sample preparation for compound specific C isotope analysis*

5
6
7 178 2.5.1 *Molecular sieves*

8
9
10 179 Approximately 1.2 mL of 5A^o molecular sieve (Sigma Aldrich) was placed into 4 mL
11
12 180 screwcap vials and activated overnight at 250 °C. Saturate fractions were washed into the
13
14 181 vials with cyclohexane (Mallinckrodt, UltiMAR grade). After agitation with a vortex mixer
15
16 182 to fully wet the sieve, the vials were placed on a hotplate at 80 °C for 8 hours. After cooling,
17
18 183 the sieve - cyclohexane slurry was transferred to a small glass Pasteur pipette (0.5 cm
19
20 184 diameter) plugged with pre-extracted cotton wool and < 0.5 cm silica gel (Merck, 0.063-
21
22 185 0.200 mm). The vial was rinsed with cyclohexane, and the sieve was washed thoroughly
23
24 186 with cyclohexane to recover the branched and cyclic (B&C) fraction. The B&C fraction
25
26 187 was evaporated to dryness and weighed.
27
28
29
30
31
32

33 188 2.5.2 *Compound specific C isotope analysis using GC-IRMS*

34
35
36 189 Saturate, B&C and OSC fractions were analyzed for compound specific $\delta^{13}\text{C}$
37
38 190 measurements on a Thermo Scientific Delta V Advantage isotope ratio mass spectrometer,
39
40 191 coupled to a Trace GC Ultra via a GC Isolink and Conflo IV. Samples were dissolved in
41
42 192 hexane (Honeywell, HPLC grade), and 1 μL was injected into the split/splitless injector
43
44 193 operating in splitless mode at constant temperature of 280 °C. Helium carrier gas was used
45
46 194 at a constant flow of 1.5 mL / min. For saturate and B&C fractions, the GC column was an
47
48 195 Agilent DB-1MS ultra inert column (60m \times 250 μm \times 0.25 μm), while for OSC fractions
49
50 196 the column was an Agilent DB-5MS ultra inert column (60m \times 250 μm \times 0.25 μm). For all
51
52 197 fractions, the GC oven was held at 40 °C for 1 min after injection, then ramped at 3 °C/min
53
54 198 to 325 °C, and held for 30 min. GC column outflow passed through the GC Isolink
55
56
57
58
59
60
61
62
63
64
65

1
2
3
4 199 combustion reactor (copper oxide and nickel oxide, 1000 °C) to combust hydrocarbons to
5
6
7 200 CO₂. The CO₂ passed through the Conflo IV interface to the IRMS, which measured m/z
8
9 201 44, 45 and 46. $\delta^{13}\text{C}$ was calculated from the measured masses by Thermo Isodat software
10
11 202 and calibrated to the VPDB scale by comparison with a mixture of n-alkane standards of
12
13
14 203 known isotopic composition. All samples were measured in triplicate.

204 3. Results

205 3.1 Bulk Geochemical parameters

206 The bulk parameters (T_{max} , total organic carbon (TOC), total sulfur (TS), the S content
207 and $\delta^{34}\text{S}$ values of kerogen and pyrite, and $\delta^{13}\text{C}$ of kerogen and bitumen) of the Ghareb
208 Formation samples were previously reported by [Shawar et al. \(2018\)](#) and summarized in
209 [Table 1S](#). In short, the T_{max} ranges between 402 and 422°C ([Table 1S](#)). TOC and TS reach
210 maximum concentrations of 22.4 wt% and 2.9 wt% at depths of 420m and 393m,
211 respectively ([Table 1S](#)). The TOC and TS contents gradually decrease to minimum values
212 (7.3 wt% and 0.4 wt%, respectively) at 595m ([Table 1S](#)).

213 The S occurs predominantly as kerogen S (KS), which represents up to 92.8 wt% of the TS
214 at depth of 528m ([Table 1S](#)). Pyrite S reaches up to 28.4 wt% of the TS at 308m ([Table](#)
215 [1S](#)). The pyritic $\delta^{34}\text{S}$ values range between -39.5‰ at 308m and -9.8‰ at 420m. The $\delta^{34}\text{S}$
216 values of KS range between -8.7‰ at 450m and 3.4‰ at 265m ([Table 1S](#)). The S isotope
217 composition of all the bulk organic S phases (namely bitumen, kerogen, asphaltenes and
218 maltenes) is similar ([Shawar et al., 2018](#)). Therefore, hereafter $\delta^{34}\text{S}$ values of KS were used
219 to represent the S isotope composition of the bulk organic S.

1
2
3
4 220 The $\delta^{13}\text{C}$ values range between -29.0‰ at 420m and -29.9‰ at 308m for kerogen, and
5
6
7 221 between -29.4‰ at 420m and -31.7‰ at 450m for the bitumen (Table 1S).
8
9

10 222 *3.2 Biomarker distribution*

11
12
13 223 Pristane to phytane ratio (Pr/Ph) ranges between 0.3 at the depth of 393m to 1 at the depth
14
15 224 of 341m (Fig. 1a).
16
17

18 225 Two biomarkers (mono-, di- and trimethylated 2-methyl-2-(4,8,12-trimethyltridecyl)
19 226 chromans and perylene), that point to terrestrial contribution into the marine sediment,
20
21 227 (Aizenshtat, 1973; Tulipani et al., 2015), were detected in our studied samples. The
22
23
24
25 228 methyltrimethyltridecylchroman (MTTC) ratio (trimethyl-2-methyl-4,8,12-
26
27 229 trimethyltridecyl chroman/ mono-, di- and trimethylated 2-methyl-2-4,8,12-
28
29
30 230 trimethyltridecyl chromans) is almost constant throughout the studied section. This ratio is
31
32
33 231 around 0.9 at the depth interval of 265 to 420m (Fig. 1b). Then, it decreased deeper in the
34
35 232 section until it reached 0.7 at the depth of 595m (Fig. 1b). Perylene concentration along the
36
37
38 233 depth profile is presented in Fig. 1c. Perylene concentration increased deeper in the studied
39
40 234 section to a maximum of 1.2 $\mu\text{g}/\text{gr}$ TOC at the depth 420m and then decreased again (Fig.
41
42
43 235 1c).
44
45

46 236 Carotenoid biomarkers were also identified in the studied samples, and the most abundant
47
48
49 237 type is isorenieratane. It occurred in trace amounts, up to 0.04 $\mu\text{g}/\text{gr}$ TOC (Fig. 1d).
50

51 238 *3.3 $\delta^{13}\text{C}$ values of non-sulfurized individual organic compounds*

52
53
54
55 239 The $\delta^{13}\text{C}$ values of individual non-sulfurized organic compounds from the saturated
56
57
58 240 fraction of the Ghareb Formation samples (normal alkanes, isoprenoids, hopanes and
59
60
61
62
63
64
65

1
2
3
4 241 steranes) are presented in [Table. 1](#). $\delta^{13}\text{C}$ values of normal alkanes vary from -37‰ to -30‰
5
6
7 242 with general trend of ^{13}C enrichment as the carbon number increases ([Table. 1](#)). The $\delta^{13}\text{C}$
8
9 243 values of pristane (Pr) and phytane (Ph) show different trends throughout the studied
10
11
12 244 section ([Fig. 1a](#)). In general, Pr is enriched in ^{13}C relative to Ph by up to ~3‰ ([Fig. 1a](#);
13
14 245 [Table. 1](#)). Moreover, the $\delta^{13}\text{C}$ values of Pr are very variable, between -35‰ at 528m to -
15
16
17 246 31‰ at 341m, while the $\delta^{13}\text{C}$ values of Ph are more consistent and vary between -35.4‰
18
19
20 247 at 450m to -33.5‰ at 265m ([Fig. 1a](#); [Table. 1](#)).

21
22
23 248 In general, steranes are depleted in ^{13}C relative to the hopanes extracted from the studied
24
25
26 249 samples ([Table. 1](#)). This depletion reaches down to 7.1‰ between C_{28} sterane-2 and C_{31}
27
28 250 hopane-2 at 450m ([Table. 1](#)).

251 *3.4 Organic S compounds distribution and their associated S and C isotope composition*

252 The $\delta^{34}\text{S}$ values of kerogen and individual OSCs from aromatic fractions (ATs and BTs)
253 and detailed description of their molecular distributions were previously reported by
254 [Shawar et al. \(2020\)](#). For simplicity and ease of comparison with the C isotope data the
255 $\delta^{34}\text{S}$ values of OSCs and their molecular distribution data are presented again in this
256 manuscript ([Fig., 2a-d and 3a-d](#); [Tables 2S and 3S](#)).

257 The $\delta^{13}\text{C}$ values of bulk phases (bitumen and kerogen) and individual ATs and BTs are
258 presented in [Figs. 2e-f and 3e-f](#), respectively, and summarized in [Table. 4S](#). A detailed
259 description of $\delta^{13}\text{C}$ of different OSCs is provided in the following sections.

260 *3.4.1 $\delta^{13}\text{C}$ of OSCs from the alkylthiophenes fraction*

1
2
3
4
5
6
7
8
9
10
11
12
13
14
15
16
17
18
19
20
21
22
23
24
25
26
27
28
29
30
31
32
33
34
35
36
37
38
39
40
41
42
43
44
45
46
47
48
49
50
51
52
53
54
55
56
57
58
59
60
61
62
63
64
65

1
2
3
4 261 The $\delta^{13}\text{C}$ values of ATs are presented in Fig. 2e-f and Table. 4S and they ranged between
5
6 262 -35 to -28‰. Unlike the normal ATs, the isoprenoid ATs (such as iC_{20} thiophene and its
7
8
9 263 isomers) show a moderate change in their $\delta^{13}\text{C}$ values throughout the studied section (Fig.
10
11 264 2e and 2f). In addition, isomers of the same AT show different C isotope composition (Fig.
12
13 265 2e and 2f). ATs with methyl substituted thiophenes (m/z 111) are ^{13}C enriched relative to
14
15 266 those with non-methyl substituted isomers (m/z 97), by up to 2‰ (Fig. 2e and 2f).
16
17 267 Similarly, most of the methyl substituted ATs (m/z 111) are ^{34}S enriched relative to the
18
19 268 non-methyl substituted isomer (m/z 97) of the same AT, by up to 8‰ (Figs. 2a and 2b;
20
21 269 Table. 2S).

270 *3.4.2 $\delta^{34}\text{S}$ of OSCs from the benzothiophenes fraction*

271 BTs were also measured for their $\delta^{13}\text{C}$ values along the depth profile and presented in Fig.
272 3e-f and Table 4S. In general, most of the BTs are ^{13}C enriched relative to kerogen, bitumen
273 and to the rest of the fractions, by an average of $\sim 3\%$ (Table. 4S). The $\delta^{13}\text{C}$ values of
274 individual BTs show large variation, $\sim 8\%$ (Fig. 3e and 3f; Table 4S), while the $\delta^{34}\text{S}$ values
275 of BTs varied by up to 15‰ compared with the kerogen (Shawar et al., 2020).

278 **4. Discussion**

279 *4.1 The origin and formation pathways of alkylthiophenes in immature sediments*

280 *4.1.1 Alkylthiophenes are derived from multiple precursors and environments*

1
2
3
4 281 Isoprenoid based ATs, such as iC₂₀ thiophenes show a moderate change in their $\delta^{13}\text{C}$ values
5
6 282 relative to the normal (linear) ATs, throughout the studied section (Fig. 2e and 2f). In
7
8 283 addition, isoprenoid ATs are generally ^{13}C and ^{34}S depleted relative to normal ATs, down
9
10 284 to ~5‰ and ~12‰ respectively (as is shown for iC₂₀, nC₁₉ and nC₁₈ thiophenes in Fig. 4 a
11
12 285 and b, and in more detail in Tables. 2S and 4S). This can be attributed to the synthesis of
13
14 286 isoprenoid and normal lipids through different biosynthetic pathways (Chikaraishi et al.,
15
16 287 2004). Moreover, the difference in $\delta^{13}\text{C}$ values of normal and isoprenoid ATs may suggest
17
18 288 that isoprenoid and normal ATs are generated by different organisms that occur in different
19
20 289 parts of the water column and thus experience different environmental conditions.
21
22 290 Subsequently, normal and isoprenoid lipids might have different functionalities and thus
23
24 291 undergo different sulfurization pathways that govern the variation in their S isotope
25
26 292 composition.
27
28
29
30
31
32
33

34 293 Isoprenoid ATs have similar $\delta^{13}\text{C}$ values to those of steranes (e.g., C₂₇ sterane; blue shaded
35
36 294 area in Fig. 5a; Tables 1 and 4S), while $\delta^{13}\text{C}$ values of normal ATs overlap with the range
37
38 295 of hopanes (e.g., C₃₁ hopane; blue shaded area in Fig. 5b; Tables 1 and 4S). These
39
40 296 observations further support previous suggestions that the carbon skeleton of isoprenoid
41
42 297 ATs mainly comes from photosynthetic organisms (or heterotrophs that feed on
43
44 298 phototrophs) that represent the upper part of the water column environment (Sinninghe
45
46 299 Damsté et al., 1986; Kohnen et al., 1990b; Grice and Brocks, 2011). Normal ATs may
47
48 300 originate mainly from prokaryotic lipids that represent the lower part of the water column
49
50 301 environment (Grice and Brocks, 2011).
51
52
53
54
55
56

57 302 Interestingly, there are differences of up to 2‰ and 8‰ in C and S isotope composition,
58
59 303 respectively, of different isomers for the same AT (Figs. 6a and b; Tables. 2S and 4S). This
60
61
62
63
64
65

1
2
3
4 304 consistent enrichment in ^{13}C and ^{34}S in *most* of the methylated ATs (m/z 111) relative to
5
6 305 the non-methylated (m/z 97), may point for different precursors and/or functionality with
7
8
9 306 different $\delta^{13}\text{C}$ values. This precursor/functionality difference might also change their
10
11
12 307 reactivity and thus their sulfurization order which in turn may affect their $\delta^{34}\text{S}$ values.
13

14 308 *4.1.2 Formation processes of Alkylthiophenes*

15
16
17
18 309 The formation processes of both isoprenoid and normal ATs as summarized in [Fig. 7](#) are:

19
20 310 I) direct formation of ATs, without the need of thermal alteration, by S incorporation into
21
22
23 311 unsaturated functionalized organic compounds (path I in [Fig.7](#)), II) thermal alteration
24
25
26 312 through either aromatization of alkylthiolanes that formed in early diagenesis or thermal
27
28 313 decomposition of S cross linked macromolecules (path II in [Fig.7](#)).
29
30

31 314 I) Do Alkylthiophenes form directly at low temperature in recent sediments?
32

33
34 315 Alkylthiophenes were observed in recent sediments, and immature rocks ([Brassell et al.,](#)
35
36 316 [1986; Barbe et al., 1990; Kenig and Huc, 1990; Grimalt et al., 1991; Hartgers et al., 1997;](#)
37
38
39 317 [Zhang et al., 2011](#)). Consequently, several studies have suggested that ATs formed directly
40
41 318 (Path I in [Fig. 7](#)) as a result of S incorporation into unsaturated functionalized organic
42
43
44 319 compounds at low temperatures ([Sinninghe Damsté et al., 1987; 1989; Fukushima et al.,](#)
45
46 320 [1992; Adam et al., 1993](#)).
47

48
49 321 Alongside the diagenetic formation pathways discussed above, it has been noted that ATs
50
51
52 322 can be formed artificially in the injector of the GC as rearrangement of precursors with S
53
54
55 323 functionalities, including S cross-linked oligomers or polymers ([Krein, 1993; Krein and](#)
56
57 324 [Aizenshtat, 1994](#)). This may result in erroneous identification of alkylthiophenes in sulfur
58
59 325 rich samples. To avoid this, a chemical cleavage of S-S and C-S bonds and their subsequent
60
61
62
63
64
65

1
2
3
4 326 methylation (e.g. MeLi/MeI treatment) is needed prior to GC analysis (Kohnen et al., 1991;
5
6 327 Krein and Aizenshtat, 1994).
7
8
9
10 328 Laboratory experiments have shown that *direct* formation of ATs requires specific
11
12 329 conditions, which are, in most cases, irrelevant to normal marine conditions, such as
13
14 330 acidic/very basic catalysis, use of organic solvents and often mild heating (LaLonde et al.,
15
16 331 1987; de Graaf et al., 1992; Fukushima et al., 1992; Krein and Aizenshtat, 1993; Rowland
17
18 332 et al., 1993). The main sulfurized product from laboratory experiments executed under
19
20 333 marine-relevant conditions are S cross-linked macromolecules, or thiol and sulfide
21
22 334 monomers, rather than ATs (Krein and Aizenshtat, 1994; Schouten et al., 1994; Krein and
23
24 335 Aizenshtat, 1995; Amrani et al., 2006). ATs were generated only after mild heating of such
25
26 336 “kerogen like” S cross-linked macromolecules (Krein and Aizenshtat, 1994; Schouten et
27
28 337 al., 1994; Amrani et al., 2006). This suggests that the dominant formation process of ATs
29
30 338 in marine sediments is macromolecular formation rather than direct formation. This may
31
32 339 suggest that ATs are generated after several diagenetic processes and mild thermochemical
33
34 340 alteration of the sulfurized lipids or precursors (path II in Fig.7). We cannot however
35
36 341 neglect the possibility of direct formation of alkylthiophenes from specific (e.g.,
37
38 342 multifunctional) structures and/or environmental conditions.

343 II) Do alkylthiophenes in immature sediments indicate that thermochemical
344 alterations started during the diagenetic stage?

345 The Ghareb Formation samples used in this study are considered to be thermally immature
346 with a T_{max} range of 402-422° C (Table. 1S) (Shawar et al., 2018; 2020). However, our
347 samples are rich in S (kerogen type IIS), which can facilitate and catalyze early
348 thermochemical alterations of sedimentary OM (Baskin and Peters, 1992). Baskin and

1
2
3
4 349 Peters (1992) have shown that thermal maturity parameters, such as T_{\max} , are negatively
5
6 350 correlated with the S/C ratio of the kerogen. As the S content in OM increases, thermal
7
8
9 351 alteration of OM starts at milder thermal stress. Further evidence is found in a recent study
10
11 352 conducted by Siedenberg et al., (2018) on immature kerogen type IIS samples from the
12
13
14 353 Jordanian Ghareb Formation, with T_{\max} range (397-423°C) similar to that of our studied
15
16 354 samples (402-422°C; Shavar et al., 2018). Siedenberg et al. (2018) showed an increase in
17
18
19 355 $\delta^{34}\text{S}$ values of bulk phases with increasing thermal maturation (represented by T_{\max} values).
20
21 356 This was attributed to the release of ^{34}S depleted H_2S during early thermal decay of organic
22
23 357 sulfur and reincorporation of this S to form a catagenetic pyrite which is ^{34}S -enriched
24
25
26 358 relative to the primary pyrite (Siedenberg et al., 2018). Koopmans et al. (1996b and 1998)
27
28
29 359 have shown that ATs are formed/released from kerogen as a result of mild artificial thermal
30
31 360 maturation of sulfur-rich rocks. Moreover, Krein and Aizenshtat (1995) and Amrani et al.
32
33 361 (2006) showed that ATs were produced after heating of S cross-linked synthetic
34
35 362 macromolecules at 160-200 ° C for 48 hr. These parameters are equivalent to Easy R_o of
36
37
38 363 up to 0.32% and T_{\max} of 415° C according to a simplified kinetic model (Sweeney and
39
40
41 364 Burnham, 1990; Jarvie et al. 2001). These calculated thermal maturation values represent
42
43 365 thermally immature levels (Peters and Cassa, 1994). The fact that laboratory experiments
44
45
46 366 showed that ATs could be formed as a result of mild thermal stress (low calculated T_{\max}
47
48 367 ~415° C) may substantiate that in S rich immature sedimentary rocks thermochemical
49
50
51 368 processes for ATs formation can start already during the diagenesis stage. This in turn
52
53 369 might explain the existence of ATs, generated mainly as a result of mild thermochemical
54
55
56 370 alteration of S cross-linked macromolecules, in immature sedimentary rocks from the
57
58 371 Ghareb Formation.
59
60
61
62
63
64
65

1
2
3
4 372 Further support for the mild thermochemical formation of ATs in the Ghareb Formation is
5
6 373 provided by the S isotope values of these compounds. When ATs are formed during
7
8
9 374 advanced thermochemical maturation the variation in their $\delta^{34}\text{S}$ values decreases to $<5\%$,
10
11 375 as a result of S isotope homogenization (Amrani et al., 2006; Ellis et al., 2017; Rosenberg
12
13
14 376 et al., 2017). However, Shavar et al. (2020) reported large variation, $\sim 15\%$, in S isotope
15
16 377 composition of individual ATs extracted from the Ghareb Formation. Moreover, they have
17
18
19 378 shown that there is no correlation in the *variation* in $\delta^{34}\text{S}$ values of different OSCs and T_{max}
20
21 379 (Shavar et al., 2020). These observations are consistent with the studied samples having
22
23
24 380 not experienced *advanced* thermal alterations, hence the thermal alteration needed for AT
25
26 381 formation is very mild. Moreover, it seems that these mild thermochemical alterations
27
28
29 382 facilitate AT formation with only minor effects on the original S isotope composition of
30
31 383 their precursors (e.g., macromolecular fraction). Therefore, the $\delta^{34}\text{S}$ and $\delta^{13}\text{C}$ variations of
32
33
34 384 ATs in Fig. 4, Tables 2S and 4S, represents differences in the C and S isotope composition
35
36 385 of their original precursors or the kerogen they were generated from, rather than thermal
37
38
39 386 alterations.

40
41
42 387 The general trend of ^{13}C in specific ATs (aromatic compounds) with the increase of T_{max}
43
44 388 of the studied samples provides another insight to this early and mild thermochemical
45
46
47 389 alteration pathway of their formation (Fig. 8). Thermal alteration studies, under laboratory
48
49 390 stimulation and natural conditions, have shown that the produced organic compounds
50
51 391 become ^{13}C -enriched with increasing thermal alteration, relative to their immature specific
52
53
54 392 fraction (Galimov and Simoneit, 1982; Sofer, 1984; Clayton and Bjorøy, 1994). Detailed
55
56 393 studies have reported that at initial stages of thermal alteration the organic compounds
57
58
59 394 become depleted in ^{13}C relative to their immature specific fraction and relative to the
60
61
62
63
64
65

1
2
3
4 395 kerogen they were generated from (Hill et al., 2003; Tocque et al., 2005). Different
5
6 396 fractions respond differently to the increase in thermal alteration (Galimov, 2006). In
7
8
9 397 addition, it was mentioned that the change in $\delta^{13}\text{C}$ values of organic compounds from
10
11 398 different fractions/families with thermal maturation is affected by other factors such as the
12
13
14 399 kerogen type and OM origin (Lorant et al., 1998; Hill et al., 2003). As the thermal
15
16 400 maturation increases, the $\delta^{13}\text{C}$ of the generated compounds (e.g., saturates) homogenize
17
18
19 401 while the $\delta^{13}\text{C}$ values of kerogen do not change significantly (Lewan, 1983; Clayton and
20
21 402 Bjorøy, 1994; Whiticar, 1996). This may suggest that the difference between $\delta^{13}\text{C}$ values
22
23
24 403 of the released compounds and the kerogen should decrease with increasing T_{max} . This
25
26 404 phenomenon can be observed in the studied system as presented in Fig. 9 a and b. The
27
28
29 405 difference between $\delta^{13}\text{C}$ values of organic compounds and their kerogen normalizes the
30
31 406 effect of the OM origin on the $\delta^{13}\text{C}$ values of the organic compounds. Thus, the general
32
33 407 trend of ^{13}C depletion in saturated and AT fractions with increasing T_{max} results mainly
34
35 408 from thermochemical alterations (Fig. 9a and b). This trend is not observed in the BT
36
37 409 fraction and this could be attributed to the increased thermal stability of BTs compared to
38
39 410 saturates and ATs (Fig. 9c). Thus, diagenetic thermochemical alteration is not enough to
40
41 411 homogenize their $\delta^{13}\text{C}$ values.
42
43
44
45
46

47
48 412 In terms of S isotopes, it has been shown that the thermal decomposition of S cross-linked
49
50 413 macromolecular fractions (kerogen, bitumen etc) at early thermal maturation is associated
51
52 414 with relatively small S isotope fractionation (Amrani et al., 2005). The released ATs have
53
54 415 similar $\delta^{34}\text{S}$ relative to the source kerogen (Rosenberg et al., 2017). Therefore, it is likely
55
56 416 that the ATs in the Ghareb Formation were generated *mainly* by early thermochemical
57
58 417 alteration of S cross linked macromolecules and possibly, also, through aromatization of
59
60
61
62
63
64
65

1
2
3
4 418 alkylthiolanes that formed during early diagenesis (Path II in Fig. 7) (Schmid et al., 1987;
5
6 419 Sinninghe Damsté et al., 1987; Payzant et al., 1989; Krein, 1993; Krein and Aizenshtat,
7
8
9 420 1994; Koopmans et al., 1996b; 1998). Such early thermal maturation can occur as long as
10
11 421 the precursors of the ATs contain the appropriate functional groups (e.g., double bonds)
12
13 422 and abundant reduced S. Therefore, ATs can be formed in high concentrations even during
14
15
16 423 the diagenesis stage within immature sedimentary rocks.
17
18

19 424 *4.2 The origin and formation pathways of BTs in immature sedimentary rocks*

20
21
22 425 A homologue series of benzothiophenes (BTs), C₀-C₅ BTs, were identified in our core
23
24 426 samples from the Shefela Basin (Fig. 5b in Shavar et al., 2020). Moreover, BTs were the
25
26 427 most abundant OSC group in the bitumen (Fig. 3c-d; Table. 3S). Unlike ATs, they are not
27
28 428 found in recent sediments and rarely in immature rocks (Perakis 1986; Sinninghe Damsté
29
30 429 et al., 1989a; Shavar et al., 2020). The origin of these compounds in oils and sedimentary
31
32 430 rocks is debated but it is suggested they are formed by thermal alteration processes
33
34 431 (Aizenshtat et al., 1995). Indeed, BTs are used as thermal maturation tracers (Radke, 1988;
35
36 432 Sinninghe Damsté et al., 1988; Sinninghe Damsté and de Leeuw, 1990; Chakhmakhchev
37
38 433 and Suzuki, 1995). Therefore, their high abundance in an immature source rock is not well
39
40 434 understood and may suggest that thermochemical processes needed for their formation can
41
42 435 occur already in the diagenesis stage. Another possibility is that there are some other,
43
44 436 unknown processes that may form BTs with no thermochemical processes (i.e. “direct
45
46 437 formation”).
47
48
49
50
51
52

53
54
55 438 In this section we consider three possible hydrocarbon sources and five possible formation
56
57 439 pathways for BTs, as illustrated in Fig. 10 and described below:
58
59
60
61
62
63
64
65

1
2
3
4 440 I) Isoprenoid quinones (biosynthetic BTs): defunctionalization of this biological
5
6 441 molecule will lead to the formation of BT (path I in Fig. 10).

7
8
9 442 II) Alkylthiophenes can form BTs according to the following pathways:

10
11 443 a) High temperature cyclization and aromatization of saturated
12
13 444 alkylthiophenes (Schmid et al., 1987; Eglinton et al., 1990; Sinnighe
14
15 445 Damsté et al., 1990) (path IIa in Fig. 10).

16
17
18 446 b) Cyclization of polyunsaturated ATs under mild thermal stress (Aizenshtat
19
20 447 et al., 1995) (path IIb in Fig. 10).

21
22
23 448 III) Aromatic compounds (such as terrestrial material or aromatic carotenoids;
24
25 449 namely isorenieratene) or alkylcyclohexanes (such as non-aromatic
26
27 450 carotenoids; namely α -carotene, β -carotene and γ -carotene) can form BTs
28
29 451 according to the following pathways:

30
31
32 452 a) High temperature S incorporation and cyclization of aromatic
33
34 453 nonfunctionalized compounds (Pryor, 1962; Przewocki et al., 1984) (path
35
36 454 IIIa in Fig. 10).

37
38
39 455 b) S incorporation into polyunsaturated/ functionalized aromatic compounds
40
41 456 or into alkylcyclohexanes and subsequent aromatization under mild thermal
42
43 457 stress (path IIIb in Fig. 10).

44
45
46
47
48
49 458 *4.2.1. Benzothiophenes generated mainly from carotenoids and/or terrestrial compounds*

50
51
52 459 The $\delta^{13}\text{C}$ values of BTs show a wide variation, up to $\sim 8\%$, which suggests multiple sources
53
54 460 (Fig. 3e and 3f). One of the possible sources for BT in organic rich sediments is isoprenoid
55
56 461 quinones (such as caldariellaquinone) that already have BT in their structure (Path I in Fig.
57
58 462 10). It was reported that there is a range of archaea that biosynthesize isoprenoid quinones
59
60
61
62
63
64
65

1
2
3
4 463 as a constituent of their plasma membrane (De Rosa et al., 1977; Collins and Langworthy,
5
6 464 1983; Nowicka and Kruk, 2010). These compounds participate in electron transfer during
7
8
9 465 chemosynthetic oxidation of S compounds and aerobic respiration (De Rosa et al., 1977).
10
11 466 Defunctionalization of isoprenoid quinones (removing the carbonyl groups) and cleavage
12
13
14 467 of their side chain, during diagenesis, yields alkylated benzothiophenes (path I in Fig. 10)
15
16 468 (De Rosa et al., 1977; Collins and Langworthy, 1983).
17
18

19 469 Although this pathway does not require thermal alteration, there are several arguments
20
21
22 470 against this possibility. First, these compounds (S-containing isoprenoid quinones such as
23
24 471 caldariellaquinone) occur mainly in archaea that lives in harsh conditions (acidophilic and
25
26 472 thermophilic archaea) (Collins and Langworthy, 1983; Lübben, 1995). It was reported that
27
28
29 473 the optimal conditions for their growth is pH of 1-3.5 and/or high temperatures of 70-95° C
30
31
32 474 (Collins and Langworthy, 1983). However, there is no evidence that the studied samples
33
34 475 were deposited under such harsh conditions (Almogi-Labin et al., 1993; Eshet et al., 1994;
35
36 476 Eshet and Almogi-Labin, 1996; Ashckenazi-Polivoda et al., 2011; Meilijson et al., 2014;
37
38 477 2015). Second, since BTs generated from quinones are biosynthetic, they should contain
39
40
41 478 biogenic S (assimilatory S) with similar $\delta^{34}\text{S}$ to that of the marine sulfate at that time, ~ 17-
42
43 479 20‰, (Claypool et al., 1980; Amrani, 2014) and thus isotopically heavier than the observed
44
45
46 480 $\delta^{34}\text{S}$ values of BTs from the studied section (-11‰ to 7‰; Fig. 3a and 3b). Therefore, the
47
48
49 481 BTs in the Ghareb samples are mostly the result of secondary sulfurization during early
50
51 482 diagenesis and there is no support for a significant contribution of biosynthetic BTs in the
52
53
54 483 studied samples.
55

56
57 484 Other possible precursors for BTs in sediments are lipids that underwent sulfurization to
58
59 485 firstly form ATs, and then subsequent cyclization and aromatization to form BTs (Schmid
60
61
62
63
64
65

1
2
3
4 486 et al., 1987; Eglinton et al., 1990;) (path IIa in Fig. 10). In specific cases when the AT side
5
6 487 chain is unsaturated and there is appropriate space between these double bonds, BTs will
7
8
9 488 form as a result of side chain cyclization, without the need of further aromatization (Schmid
10
11 489 et al., 1987; Eglinton et al., 1990) (path IIb in Fig. 10). BTs generated in this pathway
12
13
14 490 should have $\delta^{13}\text{C}$ values similar to ATs since cyclization/ aromatization is associated with
15
16 491 no or small depletion in ^{13}C (up to 1.2‰) (Sofer, 1984; Freeman, 1991; Simoneit et al.,
17
18
19 492 1993; Freeman et al., 1994). However, $\delta^{13}\text{C}$ values of BTs, in general, are heavier than
20
21 493 those of the ATs by up to 8‰ at 308m and an average of $\sim 3\%$ (Table. 4S). This in turn
22
23 494 suggests that cyclization and aromatization of ATs does not seem to be the *major* route for
24
25 495 BTs formation in our case. However, it is possible that BTs derived predominantly from
26
27 496 specific biological precursors which are different from those leading to ATs. BTs and ATs
28
29 497 that are derived from different lipid precursors will have different C isotope signatures.
30
31
32 498 Thus, the possibility of BT formation from ATs (especially unsaturated ATs; path IIb in
33
34 499 Fig. 10) cannot be completely excluded.

35
36
37
38
39 500 One of the most likely hydrocarbon source for BTs, in the studied section, seem to be
40
41 501 naturally occurring (or biosynthetic) aromatic compounds. In such cases the addition of S
42
43 502 into the side chain of the aromatic compounds or alkyl cyclohexane can facilitate
44
45 503 cyclization and aromatization to yield BTs (Path IIIa and b in Fig. 10).

46
47
48
49 504 Here we propose two possible sources for the aromatic/ alkyl cyclohexane compounds that
50
51 505 formed BTs in the Ghareb Formation: lignin (terrestrial source) and carotenoids (marine
52
53 506 source). Evidence for terrestrial contribution into the Ghareb Formation samples was found
54
55 507 in $\delta^{13}\text{C}$ values of isoprenoids and in the existence of some terrestrial biomarkers. The $\delta^{13}\text{C}$
56
57 508 values of Pr and Ph show differ by up to 3‰ throughout the studied section (Fig. 1a). This
58
59
60
61
62
63
64
65

1
2
3
4 509 suggests that they generated from different sources, most likely that there was a terrestrial
5
6
7 510 contribution for Pr (Freeman et al., 1990; Van Kaam-Peters et al., 1998). In addition, the
8
9
10 511 general trend of $\delta^{13}\text{C}$ values of normal alkanes increases with the carbon number (Table.
11
12 512 1). This in turn further support a terrestrial contribution into the OM extracted from the
13
14 513 studied samples (Murray et al., 1994).

15
16
17 514 Recent studies suggested that methyltrimethyltridecylchromane (MTTCs), biomarkers
18
19
20 515 that have been identified in our samples (Fig. 1b), might be related to terrigenous or higher
21
22 516 plant input (Tulipani et al., 2015). Other terrestrial biomarkers, such as perylene, were also
23
24
25 517 detected in the Ghareb samples (Fig. 1c). However, the perylene concentration is very low,
26
27 518 up to 1.2 $\mu\text{g}/\text{gr}$ TOC, relative to the BTs concentration of up to 60 $\mu\text{g}/\text{gr}$ TOC (Figs. 1c and
28
29
30 519 4c). This may be because our samples are immature and most of these biomarkers are still
31
32 520 linked to kerogen and polar fractions (Grice et al., 2009). These biomarkers are evidence
33
34
35 521 for terrestrial input during the deposition of the Ghareb Formation and therefore the
36
37 522 relevance of path IIIb (Fig. 10) for the formation of BTs in our samples. Organic
38
39
40 523 compounds from terrestrial origin are believed to be ^{13}C enriched by ~3-5‰, relative to
41
42 524 those from marine origin (Galimov, 2006; Grice et al., 2007). This enrichment is consistent
43
44
45 525 with the enrichment in ^{13}C of BTs, ~3‰ in average, relative to the rest of the organic
46
47 526 compounds of the Ghareb samples (Fig. 11; Tables 1 and 4S).

48
49
50 527 Another possible precursor from which BTs can be generated are aromatic carotenoids.
51
52 528 Carotenoids vary in their C isotope composition according to their synthetic pathways
53
54
55 529 (Grice and Brocks, 2011; Holman and Grice, 2018). For example, it was reported that β -
56
57
58 530 isorenieratane and β -carotane (the dominant carotenoid forms; ~-26‰), are ^{13}C -depleted
59
60 531 relative to isorenieratene produced by chlorobi (~15‰) (Koopmans et al., 1996a; Peters et

1
2
3
4 532 [al., 2005](#)). In general, chlorobi-derived carotenoids are ^{13}C -enriched relative to the rest of
5
6 533 marine biomass because of their photosynthetic pathway that takes place via the reverse
7
8
9 534 TCA cycle ([Quandt et al., 1977](#); [Sirevag et al., 1977](#); [Summons and Powell, 1986; 1987](#);
10
11 535 [Grice et al., 1996](#); [Koopmans et al., 1996a](#); [Grice et al., 1997](#)).

12
13
14 536 Thus, if BTs are generated from aromatic and non-aromatic (chlorobi-derived) carotenoids,
15
16 537 they should have heavier $\delta^{13}\text{C}$ values relative to the rest of marine-sourced OM. Indeed,
17
18
19 538 the BTs averaged $\delta^{13}\text{C}$ values is $\sim -28\text{‰}$ while the rest of the OM is $\sim -33\text{‰}$ which support
20
21
22 539 this hypothesis ([Tables 1 and 4S](#)). Previous studies have shown that carotenoids can
23
24 540 diagenetically transform to a wide range of products. Carotenoids transformation processes
25
26 541 include cleavage, double bond oxidation, migration, aromatization, sulfurization, and
27
28
29 542 polymerization ([Sinninghe Damsté et al., 1993](#); [Van Kaam-Peters and Sinninghe Damsté,](#)
30
31 543 [1997](#); [Hebting et al., 2006](#); [French et al., 2015](#)). Sulfurization during early diagenesis could
32
33 544 result in the formation of a thiophenic ring in carotenoids ([Koopmans et al. 1996a](#), [Van](#)
34
35 545 [Kaam-Peters and Sinninghe Damsté, 1997](#)). Subsequent cyclization of the unsaturated side
36
37 546 chain may lead to BT formation similar to path IIb in [Fig. 10](#). In non-aromatic carotenoids,
38
39
40 547 such as β -carotenes, the formation of a thiophenic ring and subsequent aromatization of
41
42
43 548 the cyclohexane may generate BTs. Subsequent cleavage of C-C bonds of the sulfurized
44
45
46 549 and unsaturated carotenoid is expected to occur relatively easily, ([Ishiwatari et al., 1990](#)),
47
48
49 550 and generate alkylated BTs even under low temperatures (path IIIb in [Fig. 10](#)).

50
51
52 551 In summary, since our studied samples of the Ghareb Formation are marine sedimentary
53
54 552 rocks, it is logical to assume that the major precursor for BTs formation is marine derive
55
56
57 553 (carotenoids) rather than terrestrial material. The abundance of the appropriate precursor(s)

1
2
3
4 554 for BTs formation is an important factor governing their occurrence in immature
5
6 555 sedimentary rocks.
7
8

9
10 556 *4.2.2 Benzothiophene formation pathways*
11

12
13 557 The sulfurization of biosynthetic aromatic and alkyl cyclohexane compounds (e.g. lignin,
14
15 558 aromatic and non-aromatic carotenoids) can occur by two different pathways, depending
16
17 559 on whether they contain functional groups (path III a and b in Fig. 10).
18
19

20
21 560 The first pathway, which requires high temperature, is S reincorporation and cyclization in
22
23 561 alkyl aromatic compounds (Pryor, 1962; Przewocki et al., 1984) (path IIIa in Fig. 10). The
24
25 562 S, incorporated into nonfunctionalized aromatic compounds, is released from thermal
26
27 563 decomposition of macromolecular fractions (Przewocki et al., 1984). It was reported that a
28
29 564 major product of this process is S-containing polymers rather than free BTs, and BTs will
30
31 565 be obtained after heating to elevated temperatures that facilitate the S incorporation into
32
33 566 *nonfunctionalized* aromatic compounds (Toland et al., 1958; Toland, 1961; Pryor, 1962;
34
35 567 Przewocki et al., 1984). However, such high temperatures are not characteristic of natural
36
37 568 sediments and geochemically plausible reactions must occur at temperature below 200° C
38
39 569 (de Roo and Hodgson, 1978). In term of S isotope composition, Shavar et al. (2020) have
40
41 570 shown that BTs extracted from the studied samples varied in their $\delta^{34}\text{S}$ values by up to
42
43 571 15‰ (Fig. 3a and 3b). This variation is significantly larger than the 2‰ reported in $\delta^{34}\text{S}$
44
45 572 values of BTs generated by artificial thermal maturation, of immature rock samples from
46
47 573 the same section as the studied samples (Rosenberg et al., 2017). Similarly, BTs in natural
48
49 574 oils that originated from the Ghareb Formation (e.g. Tamrur, Emuna) also varied by less
50
51 575 than 2‰ (Rosenberg et al., 2017). Thermal alteration of OSCs rapidly homogenizes their
52
53
54
55
56
57
58
59
60
61
62
63
64
65

1
2
3
4 576 S isotope composition (Armani et al., 2006). Thus, the large S isotope variation in our
5
6 577 samples excludes the possibility that the studied samples have exposed to high temperature
7
8
9 578 or to advanced thermal alteration processes (Shawar et al., 2020).

10
11 579 The second pathway we proposed is S reincorporation and cyclization and /or
12
13 580 aromatization in functionalized aromatic and alkyl cyclohexane compounds (path IIIb in
14
15 581 Fig. 10). The presence of functional groups facilitates S incorporation and thus the
16
17
18 582 temperature needed for BT formation will decrease. Laboratory experiments have shown
19
20
21 583 that BTs could be formed from mild thermal stress, 200° C for one week (or Easy R_o of
22
23 584 0.35% which is equivalent to T_{max} of 417° C), of a thermally labile synthetic S-S cross-
24
25 585 linked polymer (Amrani et al., 2006). It is also important to mention that this polymer was
26
27
28 586 *unsaturated* which facilitates cyclization reactions, and thus moderate thermochemical
29
30
31 587 processes during the diagenesis stage, as mentioned previously (*section 4.2*). The fact that
32
33 588 laboratory experiments by Amrani et al. (2006) showed that BTs could form at low
34
35 589 calculated T_{max}, ~417° C (similar to T_{max} of the studied samples), might explain the
36
37
38 590 existence of BTs in the immature studied sedimentary rocks from the Ghareb Formation
39
40
41 591 when unsaturated lipids are available. This in turn is consistent with our suggestion that
42
43 592 mild thermochemical alteration may occurred during diagenesis in the immature
44
45 593 sedimentary rocks from the Ghareb Formation. However, in a similar study we did on one
46
47 594 sample from the Ghareb Formation from another depositional Basin, Rotem Quarry, we
48
49
50 595 could not detect BTs in the bitumen. A similar phenomenon was observed in immature
51
52 596 kerogen type IIS from the Monterey Formation, Naples Beach (Shawar et al., 2020). This
53
54 597 is despite the fact that these samples (Monterey Formation and Rotem Quarry) have
55
56
57 598 comparable geochemical parameters (TOC, TS and T_{max}; Shawar et al., 2020). A possible
58
59
60
61
62
63
64
65

1
2
3
4 599 explanation is the hydrogen index (HI) in the Ghareb Formation, Shefela Basin (an average
5
6
7 600 of 760 mgHC/gTOC; [Shawar et al., 2018](#)) that is lower than in the Rotem Quarry (~836
8
9 601 mgHC/gTOC; [Amrani et al., 2005](#)). Thus, the Shefela basin samples are more unsaturated
10
11 602 relative to the Rotem Quarry sample, which facilitates early and mild thermochemical
12
13 603 alteration (*see section 4.2*). Similarly, the production index (PI) in the Ghareb Formation,
14
15 604 Shefela Basin (~0.02; [Shawar et al., 2018](#)) is larger than in Rotem Quarry (~0.01) and thus
16
17
18 605 there are more OSCs released from the kerogen to the bitumen of the Shefela Basin
19
20
21 606 samples. This further support the notion that the sedimentary OM from the Shefela Basin,
22
23 607 unlike the Rotem Quarry, already started a mild thermochemical alteration. This early
24
25 608 thermochemical alteration facilitated the formation of BTs, probably from the cleavage of
26
27
28 609 aromatic lipids or S cross-linked compounds with unsaturated side chains, and their
29
30
31 610 subsequent cyclization and aromatization.

32 33 34 611 **5. Conclusions**

35
36
37 612 In this study we investigated an immature organic and sulfur rich rock from the Ghareb
38
39 613 Formation, Shefela Basin, Israel. The novel combination of C and S isotope composition
40
41 614 analysis of individual OSCs improved our understanding of OSC formation processes and
42
43
44 615 environmental conditions. The main conclusions from this study are:

- 45
46
47 616 1. The consistent enrichment in ^{13}C and ^{34}S in most of the methylated ATs (m/z 111)
48
49 617 relative to the non-methylated (m/z 97), may point for different precursors and/or
50
51 618 functionality which affect their $\delta^{13}\text{C}$ values and their distribution. This might also
52
53
54 619 change their reactivity and thus their sulfurization order and associated $\delta^{34}\text{S}$ values.
55
56
57
58
59
60
61
62
63
64
65

1
2
3
4
5
6
7
8
9
10
11
12
13
14
15
16
17
18
19
20
21
22
23
24
25
26
27
28
29
30
31
32
33
34
35
36
37
38
39
40
41
42
43
44
45
46
47
48
49
50
51
52
53
54
55
56
57
58
59
60
61
62
63
64
65

- 620 2. The general trend of depletion in ^{13}C of ATs with the increase in T_{max} values suggest
621 that the ATs formed after a set of diagenetic processes and subsequent thermal
622 decomposition of sulfur cross-linked polymer (kerogen) rather than direct
623 formation. The large variation in $\delta^{34}\text{S}$ values of individual ATs (~15‰) suggest
624 that the thermal alteration needed for this process is modest and can occur during
625 diagenesis, and this is in agreement with previous studies based on laboratory
626 experiments.
- 627 3. Unusually high concentrations of BTs were found in the immature source rock of
628 the Shefela Basin. Their ^{13}C enriched and variable values are likely to be formed
629 from multiple organic compound precursors that are enriched in ^{13}C . The most
630 significant contributions to BTs in our study are the ^{13}C -enriched carotenoids and
631 terrestrial material that contain an aromatic/ cyclohexane group and unsaturation
632 and/or functional groups in the alkyl chain. The sulfurization of this alkyl chain and
633 subsequent ring closure can form BTs under mild thermal maturation. Therefore,
634 their occurrence in immature sedimentary rocks might point to the beginning of
635 thermochemical alteration during the diagenetic stage.
- 636 4. The formation of both ATs and BTs in immature sedimentary rocks results from
637 the combination of i) the availability of the appropriate precursors with
638 unsaturation/ functional groups, ii) the occurrence of di-/poly-sulfides in the
639 sedimentary organic matter, which facilitates the third factor governing the
640 formation of ATs and BTs, iii) early thermal alteration of the sedimentary OM. We
641 suggest that diagenetic (early) thermochemical alterations, needed for formation of
642 ATs and BTs, mainly changes the structural ratios within the OM but not the S

1
2
3
4 643 isotope composition, unlike catagenetic thermochemical alterations which
5
6 644 homogenize S isotopes between all structures.

7
8
9 645 5. The distribution of ATs and BTs, and their associated S isotope compositions, have
10
11 646 shown a potential to be used as a proxy for *diagenetic* thermochemical alteration.
12
13
14 647 Further studies on immature sedimentary rocks from different depositional
15
16 648 condition are needed to develop this proxy and to confirm its validity.

649 **Acknowledgments**

20
21
22 650 We are grateful to Harold Vinegar and Yuval Bartov from IEI Ltd. for providing the
23
24 651 core samples, to Xingqian Cui and Roger Summons for biomarker analysis using GC-
25
26 652 MS/MS. L.S. is grateful for PhD scholarships from the Ministry of National
27
28 653 Infrastructures, Energy and Water Resources of Israel, and the Harry and Sylvia
29
30 654 Hoffman Fund. A.A. Thanks the Israeli Science Foundation grant No. 1738/16 for
31
32 655 partial support to this study. A.H. and K.G. acknowledge the Australian Research
33
34 656 Council (ARC) for Discovery funding (DP150102235) supporting this work. K.G.
35
36 657 acknowledges the ARC for infrastructure grant LE110100119.

658 659 **References**

40
41
42 660 Adam, P., Schmid, J., Mycke, B., Strazielle, C., Connan, J., Huc, A., Riva, A., Albrecht P.,
43
44 661 1993. Structural investigation of nonpolar sulfur cross-linked macromolecules in
45
46 662 petroleum. *Geochimica Cosmochimica Acta* 57, 3395–3419.
47
48
49 663 Adam, P., Schneckenburger, P., Schaeffer, P., Albrecht, P., 2000. Clues to early diagenetic
50
51 664 sulfurization processes from mild chemical cleavage of labile sulfur-rich
52
53
54
55
56
57
58
59
60
61
62
63
64
65

1
2
3
4 665 geomacromolecules. *Geochimica Cosmochimica Acta* 64, 3485–3503.
5
6
7 666 Aizenshtat, Z., 1973. Perylene and its geochemical significance. *Geochimica*
8
9 667 *Cosmochimica Acta* 37, 559–567.
10
11
12 668 Aizenshtat, Z., Stoler, A., Cohen, Y., Nielsen, H., 1983. The geochemical sulphur
13
14 669 enrichment of recent organic matter by polysulfides in the Solar Lake. In *Advances*
15
16 670 in *Organic Geochemistry 1981*, ed. M Bjorøy, C Albrecht, C Cornford, K de Groot,
17
18 671 G Eglinton, et al., pp. 279–88.
19
20
21
22
23 672 Aizenshtat, Z., Krein, E. B., Vairavamurthy, M. A., Goldstein, T. P., 1995. Role of Sulfur
24
25 673 in the Transformations of Sedimentary Organic Matter: A Mechanistic Overview.
26
27 674 *ACS Symposium Series* 612, 16–37.
28
29
30
31 675 Almogi-Labin, A., Bein, A., Sass, E., 1993. Late Cretaceous upwelling system along the
32
33 676 Southern Tethys Margin (Israel): Interrelationship between productivity, bottom
34
35 677 water environments, and organic matter preservation. *Paleoceanography* 8, 671–690.
36
37
38
39 678 Amrani, A., Aizenshtat, Z., 2004a. Photosensitized oxidation of naturally occurring
40
41 679 isoprenoid allyl alcohols as a possible pathway for their transformation to thiophenes
42
43 680 in sulfur rich depositional environments. *Organic Geochemistry* 35, 693–712.
44
45
46
47 681 Amrani, A., Aizenshtat, Z., 2004b. Reaction of polysulfide anions with α,β unsaturated
48
49 682 isoprenoid aldehydes in aquatic media: simulation of oceanic conditions. *Organic*
50
51 683 *Geochemistry* 35, 909–921.
52
53
54
55 684 Amrani, A., Aizenshtat, Z., 2004c. Mechanisms of sulfur introduction chemically
56
57 685 controlled: $\delta^{34}\text{S}$ imprint. *Organic Geochemistry* 35, 1319–1336.
58
59
60
61
62
63
64
65

- 1
2
3
4 686 Amrani, A., Lewan, M. D., Aizenshtat, Z., 2005. Stable sulfur isotope partitioning during
5
6 687 simulated petroleum formation as determined by hydrous pyrolysis of Ghareb
7
8
9 688 Limestone, Israel. *Geochimica Cosmochimica Acta* 69, 5317–5331.
10
11
12 689 Amrani, A., Said-Ahamed, W., Lewan, M. D., Aizenshtat, Z., 2006. Experiments on $\delta^{34}\text{S}$
13
14 690 mixing between organic and inorganic sulfur species during thermal maturation.
15
16
17 691 *Geochimica Cosmochimica Acta* 70, 5146–5161.
18
19
20 692 Amrani, A., Sessions, A. L., Adkins, J. F., 2009. Compound-specific $\delta^{34}\text{S}$ analysis of
21
22 693 volatile organics by coupled GC/multicollector-ICPMS. *Analytical Chemistry* 81,
23
24 694 9027–9034.
25
26
27
28 695 Amrani, A., Deev, A., Sessions, A. L., Tang, Y., Adkins, J. F., Hill, R. J., Moldowan, J.
29
30 696 M., Wei Z., 2012. The sulfur-isotopic compositions of benzothiophenes and
31
32 697 dibenzothiophenes as a proxy for thermochemical sulfate reduction. *Geochimica*
33
34 698 *Cosmochimica Acta* 84, 152–164.
35
36
37
38
39 699 Amrani, A., 2014. Organosulfur Compounds : Molecular and Isotopic Evolution from
40
41 700 Biota to Oil and Gas. *Annual Review Earth and Planetary Sciences* 42, 733–768.
42
43
44 701 Ashckenazi-Polivoda, S., Abramovich, S., Almogi-Labin, A., Schneider-Mor, A.,
45
46 702 Feinstein, S., Püttmann, W., Berner, Z., 2011. Paleoenvironments of the latest
47
48 703 Cretaceous oil shale sequence, Southern Tethys, Israel, as an integral part of the
49
50 704 prevailing upwelling system. *Palaeogeography Palaeoclimatology Palaeoecology*
51
52 705 305, 93– 108.
53
54
55
56
57 706 Barakat, A. O., Rullkötter J., 1995. Extractable and bound fatty acids in core sediments
58
59 707 from the Nördlinger Ries, southern Germany. *Fuel* 74, 416–425.
60
61
62
63
64
65

1
2
3
4
5
6
7
8
9
10
11
12
13
14
15
16
17
18
19
20
21
22
23
24
25
26
27
28
29
30
31
32
33
34
35
36
37
38
39
40
41
42
43
44
45
46
47
48
49
50
51
52
53
54
55
56
57
58
59
60
61
62
63
64
65

708 Barbe, A., Grimalt, J. O., Pueyo, J. J., Albaiges, J., 1990. Characterization of model
709 evaporitic environments through the study of lipid components. *Organic*
710 *Geochemistry* 16, 815–828.

711 Baskin, D., Peters, K., 1992. Early Generation Characteristics of a Sulfur-Rich Monterey
712 Kerogen. *American Association of Petroleum Geologists Bulletin* 76, 1–13.

713 Bhatti, H. N., Khera, R. A., 2012. Biological transformations of steroidal compounds: A
714 review. *Steroids* 77, 1267–1290.

715 Brassell, S. C., Lewis, C. A., de Leeuw, J. W., de Lange, F., Damsté J. S. S., 1986.
716 Isoprenoid thiophenes: novel products of sediment diagenesis? *Nature* 320, 160–162.

717 Brunner, B., Bernasconi, S. M., 2005. A revised isotope fractionation model for
718 dissimilatory sulfate reduction in sulfate reducing bacteria. *Geochimica*
719 *Cosmochimica Acta* 69, 4759–4771.

720 Canfield, D. E., 1998. A new model for Proterozoic ocean chemistry. *Nature* 396, 450–
721 452.

722 Canfield, D. E., Farquhar, J., Zerkle, A. L., 2010. High isotope fractionations during
723 sulfate reduction in a low-sulfate euxinic ocean analog. *Geology* 38, 415–418.

724 Chakhmakhchev, A., Suzuki, N., 1995. Saturate biomarkers and aromatic sulfur
725 compounds in oils and condensates from different source rock lithologies of
726 Kazakhstan, Japan and Russia. *Organic Geochemistry* 23, 289–299.

727 Chikaraishi, Y., Naraoka, H., Poulson, S., 2004. Carbon and hydrogen isotopic
728 fractionation during lipid biosynthesis in a higher plant (*Cryptomeria japonica*).

1
2
3
4
5
6
7
8
9
10
11
12
13
14
15
16
17
18
19
20
21
22
23
24
25
26
27
28
29
30
31
32
33
34
35
36
37
38
39
40
41
42
43
44
45
46
47
48
49
50
51
52
53
54
55
56
57
58
59
60
61
62
63
64
65

729 Phytochemistry 65, 323–330.

730 Christmann, C. M., 1988. Geochimie organique de phosphates et schistes bitumineux
731 marocains : etude du processus de phosphatogenese. Université Louis Pasteur
732 (Strasbourg).

733 Claypool, G. E., Holser, W. T., Kaplan, I. R., Sakai, H., Zak I., 1980. The age curves of
734 sulfur and oxygen isotopes in marine sulfate and their mutual interpretation. Chemical
735 Geology 28, 199–260.

736 Clayton, C. J., Bjorøy, M., 1994. Effect of maturity on $^{13}\text{C}/^{12}\text{C}$ ratios of individual
737 compounds in North Sea oils. Organic Geochemistry 21, 737–750.

738 Collins, M. D., Langworthy, T. A., 1983. Respiratory Quinone Composition of Some
739 Acidophilic Bacteria. Systematic and Applied Microbiology 4, 295–304.

740 de Graaf, W., Damsté, J. S. S., de Leeuw J. W., 1992. Laboratory simulation of natural
741 sulphurization: I. Formation of monomeric and oligomeric isoprenoid polysulphides
742 by low-temperature reactions of inorganic polysulphides with phytol and phytadienes.
743 Geochimica Cosmochimica Acta 56, 4321–4328.

744 de Leeuw, J. W., Sinninghe Damsté, J. S., 1990. Organic Sulfur Compounds and Other
745 Biomarkers as Indicators of Palaeosalinity. In Geochemistry of sulfur in fossile fules
746 429, 417–443.

747 De Roo, J., Hodgson G.W., 1978. Geochemical origin of organic sulfur compounds:
748 thiophene derivatives from ethylbenzene and sulfur. Chemical Geology 22, 71–78.

749 De Rosa, M., De Rosa, S., Gambacorta, A., Minale, L., Thomson, R. H., Worthington, R.

1
2
3
4
5
6
7
8
9
10
11
12
13
14
15
16
17
18
19
20
21
22
23
24
25
26
27
28
29
30
31
32
33
34
35
36
37
38
39
40
41
42
43
44
45
46
47
48
49
50
51
52
53
54
55
56
57
58
59
60
61
62
63
64
65

750 D., 1977. Caldariellaquinone, a unique benzo[b]thiophen-4,7-quinone from
751 Caldariella acidophila, an extremely thermophilic and acidophilic bacterium. Journal
752 of the Chemical Society, Perkin Transactions 1 0, 653.

753 Eglinton, T. I., Sinninghe Damsté, J. S., Kohnen, M. E. L., de Leeuw, J. W., Larter, S. R.,
754 Patience R. L., 1990. Analysis of Maturity-Related Changes in the Organic Sulfur
755 Composition of Kerogens by Flash Pyrolysis—Gas Chromatography. In
756 Geochemistry of sulfur in fossil fuels, Journal of the American Chemical Society,
757 Washington, DC, 27, 529–565.

758 Ellis, G. S., Said-Ahmad, W., Lillis, P. G., Shawar, L., Amrani, A., 2017. Effects of thermal
759 maturation and thermochemical sulfate reduction on compound-specific sulfur
760 isotopic compositions of organosulfur compounds in Phosphoria oils from the
761 Bighorn Basin, USA. Organic Geochemistry 103, 63–78.

762 Eshet, Y., Almogi-Labin, A., Bein, A., 1994. Dinoflagellate cysts, paleoproductivity and
763 upwelling systems: A Late Cretaceous example from Israel. Marine
764 Micropaleontology 23, 231–240.

765 Eshet, Y., Almogi-Labin, A., 1996. Calcareous nannofossils as paleoproductivity
766 indicators in Upper Cretaceous organic-rich sequences in Israel. Marine
767 Micropaleontology 29, 37–61.

768 Frankel, E., 2014. Lipid oxidation. The oily press, Dundee, Scotland.

769 Freeman, K., Hayes, J. M., Trendel, J. M., Albrecht P., 1990. Evidence from carbon isotope
770 measurements for diverse origins of sedimentary hydrocarbons. Nature 343, 254–256.

1
2
3
4
5
6
7
8
9
10
11
12
13
14
15
16
17
18
19
20
21
22
23
24
25
26
27
28
29
30
31
32
33
34
35
36
37
38
39
40
41
42
43
44
45
46
47
48
49
50
51
52
53
54
55
56
57
58
59
60
61
62
63
64
65

771 Freeman, K., 1991. The carbon isotopic compositions of individual compounds from
772 ancient and modern depositional environments. dissertation, Indiana University.

773 Freeman, K., Boreham, C. J., Summons, R. E., Hayes, J. M., 1994. The effect of
774 aromatization on the isotopic compositions of hydrocarbons during early diagenesis.
775 *Organic Geochemistry* 21, 1037–1049.

776 French, K. L., Rocher, D., Zumberge, J. E., Summons, R. E., 2015. Assessing the
777 distribution of sedimentary C₄₀ carotenoids through time. *Geobiology* 13, 139–151.

778 Fukushima, K., Yasukawa, M., Muto, N., Uemura, H., Ishiwatari, R., 1992. Formation of
779 C₂₀ isoprenoid thiophenes in modern sediments. *Organic Geochemistry* 18, 83–91.

780 Galimov, E.M., Simoneit, B.R.T., 1982. Geochemistry of interstitial gases in sedimentary
781 deposits of the Gulf of California. In: Curray, J.R., Moore, D.G., et al. (Eds.), *Initial*
782 *Reports of Deep Sea Drilling Project*, 64. US Government Printing Office,
783 Washington, 781–788.

784 Galimov, E. M., 2006. Isotope organic geochemistry. *Organic Geochemistry* 37, 1200–
785 1262.

786 Grice, K., Schaeffer, P., Schwark, L., Maxwell, J.R., 1996. Molecular indicators of
787 palaeoenvironmental conditions in an immature Permian shale (Kupferschiefer,
788 Lower Rhine Basin, north-west Germany) from free and S-bound lipids. *Organic*
789 *Geochemistry* 25, 131–147.

790 Grice, K., Schaeffer, P., Schwark, L., Maxwell J.R., 1997. Changes in palaeoenvironmental
791 conditions during deposition of the Permian Kupferschiefer (Lower Rhine Basin,

1
2
3
4
5
6
7
8
9
10
11
12
13
14
15
16
17
18
19
20
21
22
23
24
25
26
27
28
29
30
31
32
33
34
35
36
37
38
39
40
41
42
43
44
45
46
47
48
49
50
51
52
53
54
55
56
57
58
59
60
61
62
63
64
65

792 northwest Germany) inferred from molecular and isotopic compositions of biomarker
793 components. *Organic Geochemistry* 26, 677–690.

794 Grice, K., Schouten, S., Nissenbaum, A., Charrach, J., Sinninghe Damsté, J.S., 1998. A
795 remarkable paradox: sulfurised freshwater algal (*Botryococcus braunii*) lipids in an
796 ancient hypersaline euxinic ecosystem *Organic Geochemistry* 28,195–216.

797 Grice, K., Schouten, S., Blokker, P., Derenne, S., Largeau, C., Nissenbaum, A., 2003.
798 Structural and isotopic analysis of kerogens in sediments rich in free sulfurised
799 *Botryococcus braunii* biomarkers *Organic Geochemistry* 34, 471–482.

800 Grice, K., Backhouse, J., Alexander, R., Marshall, N., Logan, G. A., 2005. Correlating
801 terrestrial signatures from biomarker distributions , $\delta^{13}\text{C}$, and palynology in fluvio-
802 deltaic deposits from NW Australia (Triassic – Jurassic). 36, 1347–1358.

803 Grice, K., Nabbefeld, B., Maslen E., 2007. Source and significance of selected polycyclic
804 aromatic hydrocarbons in sediments (Hovea-3 well, Perth Basin, Western Australia)
805 spanning the Permian-Triassic boundary. *Organic Geochemistry* 38, 1795–1803.

806 Grice, K., Lu, H., Atahan, P., Asif, M., Hallmann, C., Greenwood, P., Maslen, E., Tulipani,
807 S., Williford, K., Dodson, J., 2009. New insights into the origin of perylene in
808 geological samples. *Geochimica Cosmochimica Acta* 73, 6531–6543.

809 Grice, K., Brocks J. J., 2011. Biomarkers (Organic, Compound-Specific Isotopes). In
810 *Encyclopedia of Earth Sciences Series Springer Netherlands*. pp. 167–182.

811 Grimalt, J. O., Yruela, I., Saiz-Jimenez, C., Toja, J., de Leeuw, J. W., Albaigés, J., 1991.
812 Sedimentary lipid biogeochemistry of an hypereutrophic alkaline lagoon. *Geochimica*

1
2
3
4
5
6
7
8
9
10
11
12
13
14
15
16
17
18
19
20
21
22
23
24
25
26
27
28
29
30
31
32
33
34
35
36
37
38
39
40
41
42
43
44
45
46
47
48
49
50
51
52
53
54
55
56
57
58
59
60
61
62
63
64
65

813 Cosmochimica Acta 55, 2555–2577.

814 Gvirtzman, Z., Said-Ahmad, W., Ellis, G. S., Hill, R. J., Moldowan, J. M., Wei, Z.,
815 Amrani, A., 2015. Compound-specific sulfur isotope analysis of thiadiamondoids of
816 oils from the Smackover Formation, USA. Geochimica Cosmochimica Acta 167,
817 144–161.

818 Hartgers, W. A., Lòpez, J. F., Sinninghe Damsté, J. S., Reiss, C., Maxwell, J. R., Grimalt
819 J. O., 1997. Sulfur-binding in recent environments: II. Speciation of sulfur and iron
820 and implications for the occurrence of organo-sulfur compounds. Geochimica
821 Cosmochimica Acta 61, 4769–4788.

822 Hayes, J. M., Freeman, K. H., Popp, B. N., Hoham, C. H., 1990. Compound-specific
823 isotopic analyses: A novel tool for reconstruction of ancient biogeochemical
824 processes. Organic Geochemistry 16, 1115-1128.

825 Hebbing, Y., Schaeffer, P., Behrens, A., Adam, P., Schmitt, G., Schneckenburger, P.,
826 Bernasconi, S. M., Albrecht, P., 2006. Biomarker evidence for a major preservation
827 pathway of sedimentary organic carbon. Science 312, 1627–1631.

828 Hill, R.J., Tang, Y., Kaplan, I., 2003. Insight into oil cracking based on laboratory
829 experiments. Organic Geochemistry 34, 1651–1672.

830 Ho, T. Y., Rogers, M. A., Drushel, H. V., Koons, C. B., 1974. Evolution of Sulfur
831 Compounds in Crude Oils. 58, 2338-2348.

832 Hofmann, I. C., Hutchison, J., Robson, J. N., Chicarelli, M. I., Maxwell, J. R., 1992.
833 Evidence for sulphide links in a crude oil asphaltene and kerogens from reductive

- 1
2
3
4 834 cleavage by lithium in ethylamine. *Organic Geochemistry* 19, 371–387.
5
6
7
8 835 Holba, A. G., Dzou, L. I., Wood, G. D., Ellis, L., Adam, P., Schaeffer, P., Albrecht, P.,
9
10 836 Greene, T., Hughes, W. B., 2003. Application of tetracyclic polyprenoids as
11
12 837 indicators of input from fresh-brackish water environments. *Organic Geochemistry*
13
14 838 34, 441–469.
15
16
17
18 839 Holman, A. I., Grice K., 2018. $\delta^{13}\text{C}$ of aromatic compounds in sediments, oils and
19
20 840 atmospheric emissions: A review. *Organic Geochemistry* 123, 27–37.
21
22
23
24 841 Hughes, W., 1984. Use of thiophenic organosulfur compounds in characterizing crude oils
25
26 842 derived from carbonate versus siliciclastic sources. In *petroleum geochemistry and*
27
28 843 *source rock potential of carbonate rocks*, 181–196.
29
30
31
32 844 Ishiwatari, M., Ishiwatari, R., Sakashita, H., Tatsumi, T., Tominaga, H., 1990. The effect
33
34 845 of preheating treatment on pyrolysis of Chlorophyll-a simulation of diagenetic
35
36 846 processes in kerogen formation. *Chemistry letters*, 19, 875–878.
37
38
39
40 847 Jarvie, D. M., Calxton, B.L., Henk, F., Breyer, J.T., 2001. Oil and shale gas from the
41
42 848 Barnett Shale, Ft, Worth Basin, Texas. *AAPG annual meeting program*, 85, A100.
43
44
45 849 Kaplan, I. R., Emery, K. O., Rittenberg, S. C., 1963. The distribution and isotopic
46
47 850 abundance of sulphur in recent marine sediments off southern California. *Geochimica*
48
49 851 *Cosmochimica Acta* 27, 297–312.
50
51
52
53 852 Kenig, F., Huc A. Y., 1990. Incorporation of Sulfur into Recent Organic Matter in a
54
55 853 Carbonate Environment (Abu Dhabi, United Arab Emirates). In pp. 170–185.
56
57
58
59 854 Kenneth, E., Peters, M. R. C., 1994. *Applied Source Rock Geochemistry: Chapter 5: Part*
60
61
62
63
64
65

1
2
3
4 855 II. Essential Elements. 77, 93–120.
5
6
7 856 Kohnen, M. E. L., Damsté, J. S. S., ten Haven, H. L., de Leeuw, J. W., 1989. Early
8
9 857 incorporation of polysulphides in sedimentary organic matter. *Nature* 341, 640–641.
10
11
12 858 Kohnen, M.E.L., Damsté, J. S. S., Kock-van, Dalen, A. C., Haven, H. L. T., Rullkötter, J.,
13
14 859 de Leeuw, J. W., 1990a. Origin and diagenetic transformations of C₂₅ and C₃₀ highly
15
16 860 branched isoprenoid sulphur compounds: Further evidence for the formation of
17
18 861 organically bound sulphur during early diagenesis. *Geochimica Cosmochimica Acta*
19
20 862 54, 3053–3063.
21
22
23 863 Kohnen, M. E. L., Sinninghe Damsté, J. S., Rijpstra, W. I. C., de Leeuw, J. W., 1990.
24
25 864 Alkylthiophenes as Sensitive Indicators of Palaeoenvironmental Changes. In
26
27 865 *Geochemistry of sulfur in fossil fuels*, 444–485.
28
29
30 866 Kohnen, M. E. L., Sinninghe Damsté, J. S., Kock-van Dalen, A. c., Jan, W. D. L., 1991. Di-
31
32 867 or polysulphide-bound biomarkers in sulphur-rich geomacromolecules as revealed by
33
34 868 selective chemolysis. *Geochimica Cosmochimica Acta* 55, 1375–1394.
35
36
37 869 Kohnen, M. E. L., Schouten, S., Damsté, J. S. S., de Leeuw, J. W., Merritt, D. A., Hayes,
38
39 870 J. M., 1992a. Recognition of paleobiochemicals by a combined molecular sulfur and
40
41 871 isotope geochemical approach. *Science* 256, 358–362.
42
43
44 872 Kohnen, M. E. L., Schouten, S., Sinninghe Damsté, J. S., de Leeuw, J. W., Merrit, D.,
45
46 873 Hayes, J. M., 1992b. The combined application of organic sulphur and isotope
47
48 874 geochemistry to assess multiple sources of palaeobiochemicals with identical carbon
49
50 875 skeletons. *Organic Geochemistry* 19, 403–419.
51
52
53
54
55
56
57
58
59
60
61
62
63
64
65

1
2
3
4
5
6
7
8
9
10
11
12
13
14
15
16
17
18
19
20
21
22
23
24
25
26
27
28
29
30
31
32
33
34
35
36
37
38
39
40
41
42
43
44
45
46
47
48
49
50
51
52
53
54
55
56
57
58
59
60
61
62
63
64
65

876 Kohnen, M. E. ., Sinninghe Damsté, J. S., Baas, M., Dalen, A. C. K., de Leeuw, J. W.,
877 1993. Sulphur-bound steroid and phytane carbon skeletons in geomacromolecules:
878 Implications for the mechanism of incorporation of sulphur into organic matter.
879 *Geochimica Cosmochimica Acta* 57, 2515–2528.

880 Kolonic, S., Sinninghe Damste, J. S., Bottcher, M. E., Kuypers, M. M. M., Kuhnt, W.,
881 Beckmann, B., Scheeder, G., Wagner, T., 2002. Geochemical characterization of
882 Cenomanian/Turonian black shales from the Tarfaya Basin (SW Morroco).
883 Relationships between palaeoenvironmental conditions and early sulphurization of
884 sedimentray organic matter. *Journal of Petroleum Geology* 25, 325–350.

885 Koopmans, M. P., Schouten, S., Kohnen, M. E. L., Sinninghe Damsté, J. S., 1996a.
886 Restricted utility of aryl isoprenoids as indicators for photic zone anoxia. *Geochimica*
887 *Cosmochimica Acta* 60, 4873–4876.

888 Koopmans, M. P., de leeuw, J. W., Lewan, M. D., Sinninghe Damste` J.S, 1996b. Impact
889 of dia- and catagenesis on sulphur and oxygen sequestration of biomarkers as revealed
890 by artificial maturation of an immature sedimentary rock. *Organic Geochemistry* 25,
891 391–426.

892 Koopmans, M. P., Irene, W., Rijpstra, C., de leeuw, J. W., Lewan, M. D., Sinninghe
893 Damste`, J.S, 1998. Artificial maturation of an immature sulfur- and organic matter
894 rich limestone from the Ghareb Formation, Jordan. *Organic Geochemistry* 27, 503–
895 521.

896 Krein, E. B., 1993. Organic sulfur in the geosphere: Analysis, structures and chemical
897 processes. In *The Chemistry of Sulphur-Containing Functional Groups* John Wiley

1
2
3
4
5
6
7
8
9
10
11
12
13
14
15
16
17
18
19
20
21
22
23
24
25
26
27
28
29
30
31
32
33
34
35
36
37
38
39
40
41
42
43
44
45
46
47
48
49
50
51
52
53
54
55
56
57
58
59
60
61
62
63
64
65

898 and Sons Inc. pp. 975–1032.

899 Krein, E. B., Aizenshtat Z., 1993. Phase Transfer-Catalyzed Reactions between
900 Polysulfide Anions and α,β -Unsaturated Carbonyl Compounds.,

901 Krein, E. B., Aizenshtat, Z., 1994. The formation of isoprenoid sulfur compounds during
902 diagenesis: simulated sulfur incorporation and thermal transformation. *Organic*
903 *Geochemistry* 21, 1015–1025.

904 Krein, E. B., Aizenshtat, Z., 1995. Proposed Thermal Pathways for Sulfur Transformations
905 in *Organic Macromolecules: Laboratory Simulation Experiments*. American
906 Chemical Society 1155, 110–137.

907 Kutuzov, I., Rosenberg, Y. O., Bishop, A., Amrani A., 2019. The origin of organic sulphur
908 compounds and their impact on the paleoenvironmental record. In *Hydrocarbons, Oils*
909 *and Lipids: Diversity, Origin, Chemistry and Fate*. Handbook of Hydrocarbon and
910 *Lipid Microbiology* (ed. H. Wilkes). Springer, Cham.

911 LaLonde, R. T., Ferrara, L. M., Hayes, M. P., 1987. Low-temperature, polysulfide
912 reactions of conjugated ene carbonyls: A reaction model for the geologic origin of S-
913 heterocycles. *Organic Geochemistry* 11, 563–571.

914 Lewan, M.D., 1983. Effects of thermal maturation on stable organic carbon isotopes as
915 determined by hydrous pyrolysis of Woodford Shale. *Geochimica Cosmochimica*
916 *Acta* 47, 1471–1479.

917 Lorant, F., Prinzhofer, A., Behar, F., Huc, A.Y., 1998. Carbon isotopic and molecular
918 constraints on the formation and the expulsion of thermogenic hydrocarbon gases.

1
2
3
4
5
6
7
8
9
10
11
12
13
14
15
16
17
18
19
20
21
22
23
24
25
26
27
28
29
30
31
32
33
34
35
36
37
38
39
40
41
42
43
44
45
46
47
48
49
50
51
52
53
54
55
56
57
58
59
60
61
62
63
64
65

919 Chemical Geology 147, 240–264.

920 Lübben, M., 1995. Cytochromes of archaeal electron transfer chains. *Biochimica et*
921 *Biophysica Acta - Bioenergetics* 1229, 1–22.

922 Machel, H. G., 2001. Bacterial and thermochemical sulfate reduction in diagenetic settings:
923 old and new insight. *Sedimentary Geology* 140, 143–75.

924 Meilijson, A., Ashckenazi-Polivoda, S., Ron-Yankovich, L., Illner, P., Alsenz, H., Speijer,
925 R. P., Almogi-Labin, A., Feinstein, S., Berner, Z., Püttmann, W., Abramovich, S.,
926 2014. Chronostratigraphy of the Upper Cretaceous high productivity sequence of the
927 southern Tethys, Israel. *Cretaceous Research* 50, 187–213.

928 Meilijson, A., Ashckenazi-polivoda, S., Illner, P., Alsenz, H., Speijer, R. P., Almogi-labin
929 A., Feinstein, S., Puttmann, W., Abramovich, S., 2015. Evidence for specific
930 adaptations of fossil benthic foraminifera to anoxic–dysoxic environments.
931 *Paleobiology* 42, 77–97.

932 Murray, A. P., Summons, R. E., Boreham, C. J., Dowling, L. M., 1994. Biomarker and n-
933 alkane isotope profiles for Tertiary oils: relationship to source rock depositional
934 setting. *Organic Geochemistry* 22.

935 Meshoulam, A., Ellis, G. S., Said Ahmad, W., Deev, A., Sessions, A. L., Tang, Y., Adkins,
936 J. F., Liu, J., Gilhooly, W. P., Aizenshtat, Z., Amrani, A., 2016. Study of
937 thermochemical sulfate reduction mechanism using compound specific sulfur isotope
938 analysis. *Geochimica Cosmochimica Acta* 188, 73–92.

939 Nowicka, B., Kruk J., 2010. Occurrence, biosynthesis and function of isoprenoid quinones.

1
2
3
4
5
6
7
8
9
10
11
12
13
14
15
16
17
18
19
20
21
22
23
24
25
26
27
28
29
30
31
32
33
34
35
36
37
38
39
40
41
42
43
44
45
46
47
48
49
50
51
52
53
54
55
56
57
58
59
60
61
62
63
64
65

940 Biochimica et Biophysica Acta – Bioenergetics 1797, 1587–1605.

941 Orr, W. L. , 1986. Kerogen/asphaltene/sulfur relationships in sulfur-rich Monterey oils.
942 Organic Geochemistry 10, 499–516.

943 Payzant, J. D., McIntyre, D. D., Mojelsky, T. W., Torres, M., Montgomery, D. S., Strausz,
944 O. P., 1989. The identification of homologous series of thiolanes and thianes
945 possessing a linear carbon framework from petroleums and their interconversion
946 under simulated geological conditions. Organic Geochemistry 14, 461–473.

947 Perakis, N., 1986. Séparation et détection sélective de composés soufrés dans les
948 fractions lourdes des pétroles. Géochimie des benzo[b]thiophènes. Ph.D.
949 dissertation, Univ. Strasbourg.

950 Peters, K. E., Cassa, M. R., 1994. Applied source rock geochemistry. In: Magoon, L. B.,
951 Dow, W. G. (Eds.), The petroleum system from source to trap. American association
952 of petroleum geologists memoir 60, 93–120.

953 Peters, K., Walters, C., Moldowan, J., 2005. The biomarker guide: biomarkers and isotopes
954 in the environment and human history. Cambridge, UK, Cambridge Uni. press.

955 Pryor, W. A., Pickering, T. L., 1962. Reactions of Radicals. Rates of Chain Transfer of
956 Disulfides and Peroxides with the Polystyryl Radical. Journal of the American
957 Chemical Society 84, 2705–2711.

958 Przewocki, K., Malinski, E., Szafranek, J., 1984. Elemental sulfur reactions with toluene,
959 dibenzyl, Z-stilbene and their geochemical significance. Chemical Geology 47, 347–
960 360.

1
2
3
4
5
6
7
8
9
10
11
12
13
14
15
16
17
18
19
20
21
22
23
24
25
26
27
28
29
30
31
32
33
34
35
36
37
38
39
40
41
42
43
44
45
46
47
48
49
50
51
52
53
54
55
56
57
58
59
60
61
62
63
64
65

961 Quandt, L., Gottschalk, G., Ziegler, H., Stichler, W., 1977. Isotopic discrimination by
962 photosynthetic bacteria. *FEMS Microbiology Letter* 1, 125–128.

963 Radke, M., 1988. Application of aromatic compounds as maturity indicators in source
964 rocks and crude oils. *Marine and Petroleum Geology* 5, 224–236.

965 Raven, M. R., Adkins, J. F., Werne, J. P., Lyons, T. W., Sessions, A. L., 2015. Sulfur
966 isotopic composition of individual organic compounds from Cariaco Basin sediments.
967 *Organic Geochemistry* 80, 53-59.

968 Rosenberg, Y. O., Meshoulam, A., Said-Ahmad, W., Shawar, L., Dror, G., Reznik, I. J.,
969 Feinstein, S., Amrani, A., 2017. Study of thermal maturation processes of sulfur-rich
970 source rock using compound specific sulfur isotope analysis. *Organic Geochemistry*
971 112, 59–74.

972 Rosenberg, Y. O., Kutuzov, I., Amrani A., 2018. Sulfurization as a preservation
973 mechanism for the $\delta^{13}\text{C}$ of biomarkers. *Organic Geochemistry* 125, 66–69.

974 Rowland, S., Rockey, C., Al-Lihaibi, S. S., Wolff, G. A., 1993. Incorporation of sulphur
975 into phytol derivatives during simulated early diagenesis. *Organic Geochemistry* 20,
976 1–5.

977 Russell, M., Hartgers, W. A., Grimalt, J. O., 2000. Identification and geochemical
978 significance of sulphurized fatty acids in sedimentary organic matter from the Lorca
979 Basin, SE Spain. *Geochimica Cosmochimica Acta* 64, 3711–3723.

980 Said-Ahmad, W., Amrani, A., 2013. A sensitive method for the sulfur isotope analysis of
981 dimethyl sulfide and dimethylsulfoniopropionate in seawater. *Rapid Communication*

1
2
3
4
5
6
7
8
9
10
11
12
13
14
15
16
17
18
19
20
21
22
23
24
25
26
27
28
29
30
31
32
33
34
35
36
37
38
39
40
41
42
43
44
45
46
47
48
49
50
51
52
53
54
55
56
57
58
59
60
61
62
63
64
65

982 Mass Spectrometry 27, 2789–96.

983 Schaeffer, P., Adam, P., Philippe, E., Trendel, J. M., Schmid, J., Behrens, A., Connan, J.,
984 Albrecht P., 2006. The wide diversity of hopanoid sulfides evidenced by the structural
985 identification of several novel hopanoid series. 37, 1590–1616.

986 Schaeffer, P., Reiss, C., Albrecht, P., 1995. Geochemical study of macromolecular organic
987 matter from sulfur-rich sediments of evaporitic origin (Messinian of Sicily) by
988 chemical degradations. Organic Geochemistry 23, 567–581.

989 Schmid, J. C., Connan, J., Albrecht, P., 1987. Occurrence and geochemical significance of
990 long-chain dialkylthiacyclopentanes. Nature 329, 54–56.

991 Schou, L., Myhr, M. B., 1988. Sulfur aromatic compounds as maturity parameters. In
992 Organic Geochemistry In Petroleum Exploration Elsevier, 61–66.

993 Schouten, S., de Graaf, W., Sinninghe Damsté, J. S., van Driel, G. B., de Leeuw, J. W.,
994 1994. Laboratory simulation of natural sulphurization: II. Reaction of multi-
995 functionalized lipids with inorganic polysulphides at low temperatures. Organic
996 Geochemistry 22, 825-834.

997 Schwark, L., Vliex, M., Schaeffer, P., 1998. Geochemical characterization of Malm Zeta
998 laminated carbonates from the Franconian Alb, SW-Germany (II). Organic
999 Geochemistry 29, 1921–1952.

1000 Scofield, A. D. L., 1990. Nouveaux marqueurs biologiques de sediments et petroles riches
1001 en soufre : identification et mode de formation. Université Louis Pasteur (Strasbourg).

1002 Shawar, L., Halevy, I., Said-Ahmad, W., Feinstein, S., Boyko, V., Kamyshny, A., Amrani,

1
2
3
4
5
6
7
8
9
10
11
12
13
14
15
16
17
18
19
20
21
22
23
24
25
26
27
28
29
30
31
32
33
34
35
36
37
38
39
40
41
42
43
44
45
46
47
48
49
50
51
52
53
54
55
56
57
58
59
60
61
62
63
64
65

1003 A., 2018. Dynamics of pyrite formation and organic matter sulfurization in organic-
1004 rich carbonate sediments. *Geochimica Cosmochimica Acta* 241, 219–239.

1005 Shawar, L., Said-Ahmad, W., Ellis, P., Amrani, A., 2020. Sulfur isotope composition of
1006 individual compounds in immature organic-rich rocks and possible geochemical
1007 implications. *Geochimica Cosmochimica Acta* 274, 20–44.

1008 Sheng, G., Fu, J., Brassell, S. C., Gowar, A. P., Eglinton, G., Sinninghe Damste`, J. S., de
1009 Leeuw, J. W., Schenck, P. A., 1987. Sulphur-containing compounds in sulphur-rich
1010 crude oils from hypersaline lake sediments and their geochemical implications.
1011 *Chinese J. Geochemistry* 6, 115–126.

1012 Siedenber, K., Strauss, H., Podlaha, O., van den Boorn, S., 2018. Multiple sulfur isotopes
1013 ($\delta^{34}\text{S}$, $\Delta^{33}\text{S}$) of organic sulfur and pyrite from Late Cretaceous to Early Eocene oil
1014 shales in Jordan. *Organic Geochemistry* 125, 29–40.

1015 Sim, M. S., Bosak, T., Ono, S., 2011. Large Sulfur Isotope Fractionation Does Not Require
1016 Disproportionation. *Science* 333, 74–77.

1017 Simoneit, B. R., Schoell, M., Dias, R. F., de Aquino Neto, F. R., 1993. Unusual carbon
1018 isotope compositions of biomarker hydrocarbons in a Permian tasmanite. *Geochimica*
1019 *Cosmochimica Acta* 57, 4205–4211.

1020 Sinninghe Damsté, J. S., ten Haven, H. L., de Leeuw, J. W., Schenck, P. A., 1986. Organic
1021 geochemical studies of a Messinian evaporitic basin, northern Apennines (Italy)—II
1022 Isoprenoid and n-alkyl thiophenes and thiolanes. *Organic Geochemistry* 10, 791–805.

1023 Sinninghe Damsté, J. S., de Leeuw, J. W., Kock-Van Dalen, A., De Zeeuw, M. A., Lange,

1
2
3
4
5
6
7
8
9
10
11
12
13
14
15
16
17
18
19
20
21
22
23
24
25
26
27
28
29
30
31
32
33
34
35
36
37
38
39
40
41
42
43
44
45
46
47
48
49
50
51
52
53
54
55
56
57
58
59
60
61
62
63
64
65

1024 F. De, Irene, W., Rijpstra, C., Schenck, P., 1987. The occurrence and identification of
1025 series of organic sulphur compounds in oils and sediment extracts. I. A study of Rozel
1026 Point Oil (U.S.A.). *Geochimica Cosmochimica Acta* 51, 2369–2391.

1027 Sinninghe Damsté, J. S., Kock-Van Dalen, A. C., de Leeuw, J. W., Schenck, P. A., 1988
1028 Identification of homologous series of alkylated thiophenes, thiolanes, thianes and
1029 benzothiophenes present in pyrolysates of sulphur-rich kerogens. *Journal of*
1030 *Chromatography A* 435, 435–452.

1031 Sinninghe Damsté, J. S., Eglinton, T. I., de Leeuw, J. W., Schenck, P. A., 1989a. Organic
1032 sulphur in macromolecular sedimentary organic matter: I. Structure and origin of
1033 sulphur-containing moieties in kerogen, asphaltenes and coal as revealed by flash
1034 pyrolysis. *Geochimica Cosmochimica Acta* 53, 873–889.

1035 Sinninghe Damsté, J. S., Rijpstra, W. I. C., de Leeuw, J. W., Schenck, P., 1989b. The
1036 occurrence and identification of series of organic sulphur compounds in oils and
1037 sediment extracts: II. Their presence in samples from hypersaline and non-hypersaline
1038 palaeoenvironments and possible application as source, palaeoenvironmental and
1039 maturity indicators. *Geochimica Cosmochimica Acta* 53, 1323–1341.

1040 Sinninghe Damsté, J. S., Rijpstra, W. I. C., Kock-van Dalen, A. C., de Leeuw, J. W.,
1041 Schenck, P. A., 1989c. Quenching of labile functionalised lipids by inorganic sulphur
1042 species: Evidence for the formation of sedimentary organic sulphur compounds at the
1043 early stages of diagenesis. *Geochimica Cosmochimica Acta* 53, 1343–1355.

1044 Sinninghe Damsté, J. S., Eglinton, T. I., Rijpstra, W. I. C., de Leeuw, J. W., 1990.
1045 Characterization of Organically Bound Sulfur in High-Molecular-Weight,

1
2
3
4
5
6
7
8
9
10
11
12
13
14
15
16
17
18
19
20
21
22
23
24
25
26
27
28
29
30
31
32
33
34
35
36
37
38
39
40
41
42
43
44
45
46
47
48
49
50
51
52
53
54
55
56
57
58
59
60
61
62
63
64
65

1046 Sedimentary Organic Matter Using Flash Pyrolysis and Raney Ni Desulfurization. In
1047 Geochemistry of sulfur in fossil fuels. 429, 486–528.

1048 Sinninghe Damsté, J. S., de Leeuw J. W., 1990. Analysis, structure and geochemical
1049 significance of organically-bound sulphur in the geosphere: State of the art and future
1050 research. *Organic Geochemistry* 16, 1077–1101.

1051 Sinninghe Damsté, J. S., Wakeham, S. G., Kohlen, M. E. L., Hayes, J. M., de Leeuw, J.
1052 W., 1993. A 6,000-year sedimentary molecular record of chemocline excursions in
1053 the Black Sea. *Nature* 362, 827–829.

1054 Sirevag, R., Buchanan, B. B., Berry, J. A., Troughton, J. H., 1977. Mechanisms of CO₂
1055 fixation in bacterial photosynthesis studied by carbon isotope fractionation technique.
1056 *Archives Microbiology* 112, 35–38.

1057 Sofer, Z., 1984. Stable Carbon Isotope Compositions of Crude Oils: Application to Source
1058 Depositional Environments and Petroleum Alteration. *American Association of
1059 Petroleum Geologists Bulletin* 68, 31-49.

1060 Soudry, D., Glenn, C. R., Nathan, Y., Segal, I., VonderHaar, D., 2006. Evolution of
1061 Tethyan phosphogenesis along the northern edges of the Arabian–African shield
1062 during the Cretaceous–Eocene as deduced from temporal variations of Ca and Nd
1063 isotopes and rates of P accumulation. *Earth-Science Review* 78, 27–57.

1064 Sweeney, J. J., Burnham, A. K., 1990. Evaluation of a simple model of vitrinite reflectance
1065 based on chemical kinetics. *American Association of Petroleum Geologists Bulletin*
1066 74, 1559–1570.

1
2
3
4
5
6
7
8
9
10
11
12
13
14
15
16
17
18
19
20
21
22
23
24
25
26
27
28
29
30
31
32
33
34
35
36
37
38
39
40
41
42
43
44
45
46
47
48
49
50
51
52
53
54
55
56
57
58
59
60
61
62
63
64
65

1067 Summons, R.E., Powell, T.G., 1986. Chlorobiaceae in Palaeozoic seas revealed by
1068 biological markers, isotopes and geology. *Nature* 319, 763–765.

1069 Summons, R.E., Powell, T.G., 1987. Identification of aryl isoprenoids in source rocks and
1070 crude oils: Biological markers for the green sulphur bacteria. *Geochimica*
1071 *Cosmochimica Acta* 51, 557–566.

1072 Ten Haven, H. L., de Leeuw, J. W., Schenck, P. A., 1985. Organic geochemical studies of
1073 a Messinian evaporitic basin, northern Apennines (Italy) I: Hydrocarbon biological
1074 markers for a hypersaline environment. *Geochimica Cosmochimica Acta* 49, 2181–
1075 2191.

1076 Tocque, E., Behar, F., Budzinski, H., Lorant F., 2005. Carbon isotopic balance of kerogen
1077 pyrolysis effluents in a closed system. *Organic Geochemistry* 36, 893–905.

1078 Tulipani, S., Grice, K., Greenwood, P. F., Schwark, L., Böttcher, M. E., Summons, R. E.,
1079 Foster C. B., 2015. Molecular proxies as indicators of freshwater incursion-driven
1080 salinity stratification. *Chemical Geology* 409, 61–68.

1081 Van Kaam-Peters, H. M. E., Sinninghe Damsté, J. S., 1997. Characterisation of an
1082 extremely organic sulphur-rich, 150 Ma old carbonaceous rock: Palaeoenvironmental
1083 implications. *Organic Geochemistry* 27, 371–397.

1084 Van Kaam-Peters, H. M. E., Rijpstra, W. I. C., de Leeuw, J. W., Sinninghe Damsté, J. S.,
1085 1998. A high resolution biomarker study of different lithofacies of organic sulfur-rich
1086 carbonate rocks of a Kimmeridgian lagoon (French southern Jura). *Organic*
1087 *Geochemistry* 28, 151–177.

1
2
3
4
5
6
7
8
9
10
11
12
13
14
15
16
17
18
19
20
21
22
23
24
25
26
27
28
29
30
31
32
33
34
35
36
37
38
39
40
41
42
43
44
45
46
47
48
49
50
51
52
53
54
55
56
57
58
59
60
61
62
63
64
65

1088 Werne, J. P., Hollander, D. J., Lyons, T. W., Damsté J. S. S., 2004. Organic sulfur
1089 biogeochemistry: Recent advances and future research directions. In sulfur
1090 biogeochemistry: past and present, 379, 135–150.

1091 Whiticar, M.J., 1996. Stable isotope geochemistry of coals, humic kerogens and related
1092 natural gases. International Journal of Coal Geology, 32, 191–215.

1093 Wortmann, U. G., Bernasconi, S. M., Böttcher, M. E., 2001. Hypersulfidic deep biosphere
1094 indicates extreme sulfur isotope fractionation during single-step microbial sulfate
1095 reduction. Geology 29, 647.

1096 Zhang, Z., Metzger, P., Sachs, J. P., 2011. Co-occurrence of long chain diols, keto-ols,
1097 hydroxy acids and keto acids in recent sediments of Lake El Junco, Galápagos Islands.
1098 Organic Geochemistry 42, 823–837.

1099 **Table and Figure captions**

1100 **Table 1** The $\delta^{13}\text{C}$ values (‰) of normal alkanes, isoprenoids, hopanes and steranes of the
1101 saturated fraction extracted from the Ghareb Formation samples.

1102 **Fig.1** Depth profiles for **a**) pristane to phytane ratio (Pr/Ph) and their $\delta^{13}\text{C}$ values (‰), **b**)
1103 methyltrimethyltridecylchromane ratio (MTTC ratio), **c**) perylene concentration ($\mu\text{g/g}$
1104 TOC) and **d**) isorenieratane concentration ($\mu\text{g/g}$ TOC) in the Ghareb Formation samples.

1105 **Fig. 2** Depth profiles for **a and b**) $\delta^{34}\text{S}$ values (‰), **c and d**) concentrations ($\mu\text{g/g}$ TOC),
1106 and **e and f**) $\delta^{13}\text{C}$ values (‰) of isoprenoid and normal alkylthiophenes, respectively,
1107 extracted from the Ghareb Formation samples. The x in C_x stands for carbon number of

1
2
3
4 1108 alkylthiophene, i and n for isoprenoid and normal respectively, T for thiophene, and HT for
5
6 1109 hopane thiophene. The numbers for the base peak (m/z) of different isomers. Figures **a-d**
7
8
9 1110 are modified after [Shawar et al. \(2020\)](#).

10
11
12 1111 **Fig. 3** Depth profiles for **a and b\delta^{34}\text{S} values (‰), **c and d**) concentrations ($\mu\text{g/gTOC}$),
13
14
15 1112 and **e and f**) $\delta^{13}\text{C}$ values (‰) of $\text{C}_1\text{-C}_3$ and $\text{C}_4\text{-C}_5$ benzothiophenic compounds (BT),
16
17
18 1113 respectively, extracted from the Ghareb Formation samples. The x in C_x stands for carbon
19
20
21 1114 number of the BT's side chain, and the numbers for different isomers. Figures **a-d** are
22
23 1115 modified after [Shawar et al. \(2020\)](#).**

24
25
26 1116 **Fig. 4** Cross plot of $\delta^{13}\text{C}$ values (‰) and $\delta^{34}\text{S}$ values (‰) of **a**) isoprenoid C_{20} thiophenes
27
28
29 1117 (iC_{20} thiophene) and normal C_{18} alkylthiophenes (nC_{18} thiophene), **b**) isoprenoid C_{20}
30
31
32 1118 thiophenes (iC_{20} thiophene) and normal C_{19} alkylthiophenes (nC_{19} thiophene) extracted
33
34
35 1119 from the Ghareb Formation samples. For simplicity only two thiophenes are presented in
36
37 1120 each sub-figure. For the complete data see Tables 2S and 4S.

38
39
40 1121 **Fig. 5** $\delta^{13}\text{C}$ values (‰) depth profiles for **a**) C_{27} sterane, methylated iC_{20} thiophene ($\text{iC}_{20}\text{T-}$
41
42
43 1122 111) and non-methylated iC_{20} thiophene ($\text{iC}_{20}\text{T-97}$), **b**) C_{31} hopane, normal alkylthiophenes
44
45
46 1123 (methylated C_{19} thiophene ($\text{C}_{19}\text{T-111}$), non-methylated C_{20} thiophene ($\text{C}_{20}\text{T-97}$) and
47
48
49 1124 methylated C_{21} thiophene ($\text{C}_{21}\text{T-111}$)) extracted from the Ghareb Formation samples. Blue
50
51
52 1125 shaded area represents the range of $\delta^{13}\text{C}$ averaged values (‰) for **a**) steranes and **b**)
53
54 1126 hopanes extracted from the Ghareb Formation samples.
55
56
57
58
59
60
61
62
63
64
65

1
2
3
4
5 1127 **Fig. 6** Cross plot of **a)** $\delta^{13}\text{C}$ values (‰) of methylated and non-methylated isoprenoid C_{20}
6
7 1128 thiophenes ($\text{iC}_{20}\text{T-111}$ and $\text{iC}_{20}\text{T-97}$), methylated and non-methylated normal C_{18}
8
9 1129 thiophenes ($\text{nC}_{18}\text{T-111}$ and $\text{nC}_{18}\text{T-97}$) **b)** $\delta^{34}\text{S}$ values (‰) of methylated and non-
10
11 1130 methylated isoprenoid C_{20} thiophenes ($\text{iC}_{20}\text{T-111}$ and $\text{iC}_{20}\text{T-97}$), methylated and non-
12
13 1131 methylated normal C_{18} thiophenes ($\text{nC}_{18}\text{T-111}$ and $\text{nC}_{18}\text{T-97}$), methylated and non-
14
15 1132 methylated C_{35} hopane thiophenes ($\text{C}_{35}\text{HT-111}$ and $\text{C}_{35}\text{HT-97}$) extracted from the Ghareb
16
17 1133 Formation samples.

18
19
20
21
22
23
24 1134 **Fig. 7** Possible formation pathways for alkylthiophene in the sediments.

25
26
27 1135 **Fig. 8.** Cross plot of T_{max} ($^{\circ}\text{C}$) versus $\delta^{13}\text{C}$ values (‰) of alkylthiophenes extracted from
28
29 1136 the Ghareb Formation samples. The x in C_x stands for carbon number of the
30
31 1137 alkylthiophenes (ATs), and the number 111 for the base peak (m/z) of ATs different isomers.
32
33 1138 The shaded area shows the general trend of depletion in ^{13}C of the ATs with the increase in
34
35 1139 T_{max} .

36
37
38
39
40
41
42 1140 **Fig. 9** Cross plot of T_{max} ($^{\circ}\text{C}$) versus the difference in $\delta^{13}\text{C}$ values (‰) between **a)**
43
44 1141 saturated compounds and kerogen, **b)** alkylthiophenes (ATs) and kerogen and **c)**
45
46 1142 benzothiophenes (BTs) and kerogen from the Ghareb Formation samples. The x in C_x
47
48 1143 stands for carbon number of the organic compound, and the numbers 111 and 97 for the
49
50 1144 base peak (m/z) of ATs different isomers. n stands for normal and T for thiophene. The
51
52 1145 arrows show the decrease in the difference between $\delta^{13}\text{C}$ values of the organic compounds
53
54 1146 from different families and the kerogen with the increase in T_{max} . BTs do not show a similar
55
56
57
58
59
60
61
62
63
64
65

1
2
3
4
5
6
7
8
9
10
11
12
13
14
15
16
17
18
19
20
21
22
23
24
25
26
27
28
29
30
31
32
33
34
35
36
37
38
39
40
41
42
43
44
45
46
47
48
49
50
51
52
53
54
55
56
57
58
59
60
61
62
63
64
65

1147 trend, and this may show that the BTs are generated at later stages of thermochemical
1148 alteration.

1149 **Fig. 10** Possible formation pathways for benzothiophenes in the sediment. Path **I** represents
1150 diagenetic alteration of isoprenoid quinones, path **IIa** high temperature cyclization and
1151 aromatization of saturated alkylthiophenes, path **IIb** cyclization of polyunsaturated
1152 alkylthiophenes under mild thermal stress, path **IIIa** high temperature S reincorporation
1153 and cyclization of aromatic non- functionalized compounds, path **IIIb** S incorporation into
1154 polyunsaturated/ functionalized aromatic compounds (from carotenoids and terrestrial
1155 matter) under mild thermal stress.

1156 **Fig. 11** Cross plot of $\delta^{13}\text{C}$ averaged values (‰) of all the benzothiophenes (BTs) versus
1157 averaged $\delta^{13}\text{C}$ values (‰) of all the saturated compounds, in blue, and all the
1158 alkylthiophenes (ATs), in yellow, extracted from the Ghareb Formation samples.

1159 **Supplementary material:**

1160 **Table 1S** The bulk parameters (T_{max} ($^{\circ}\text{C}$), total organic carbon (TOC (wt%)), total sulfur
1161 (TS (wt%)), the S content (wt% of TS) and $\delta^{34}\text{S}$ values (‰) of kerogen and pyrite, and
1162 $\delta^{13}\text{C}$ (‰) of kerogen and bitumen) of the core samples from the Ghareb Formation ([Shawar
1163 et al., 2018](#)).

1164 **Table 2S** $\delta^{34}\text{S}$ values (‰) of alkyl thiophenic (ATs), and benzothiophenic (BTs)
1165 compounds extracted from the Ghareb Formation samples. The compound names of ATs
1166 include the ion mass (m/z) in order to distinguish between different isomers. The numbers
1167 in BT names represent different isomers and not their ion mass since they have the same

1
2
3
4
5
6
7
8
9
10
11
12
13
14
15
16
17
18
19
20
21
22
23
24
25
26
27
28
29
30
31
32
33
34
35
36
37
38
39
40
41
42
43
44
45
46
47
48
49
50
51
52
53
54
55
56
57
58
59
60
61
62
63
64
65

1168 ion mass. The retention time of the compounds is reported from the GC-MC-ICPMS
1169 analyses ([Shawar et al., 2020](#)).

1170

1171 **Table 3S** Concentration ($\mu\text{g/gTOC}$) of alkyl thiophenic (ATs) and benzothiophenic (BTs)
1172 compounds extracted from the Ghareb Formation samples. The compound names of ATs
1173 include the ion mass (m/z) in order to distinguish between different isomers. The numbers
1174 in BT names represent different isomers and not their ion mass since they have the same
1175 ion mass. The retention time of the compounds is reported from the GC-MS analyses
1176 ([Shawar et al., 2020](#)).

1177 **Table 4S** $\delta^{13}\text{C}$ values (‰) of alkyl thiophenic (ATs) and benzothiophenic (BTs)
1178 compounds extracted from the Ghareb Formation samples. The compound name of ATs
1179 includes the ion mass (m/z) in order to distinguish between different isomers. The numbers
1180 in BT names represent different isomers and not their ion mass since they have the same
1181 ion mass.

1182

Fig.1

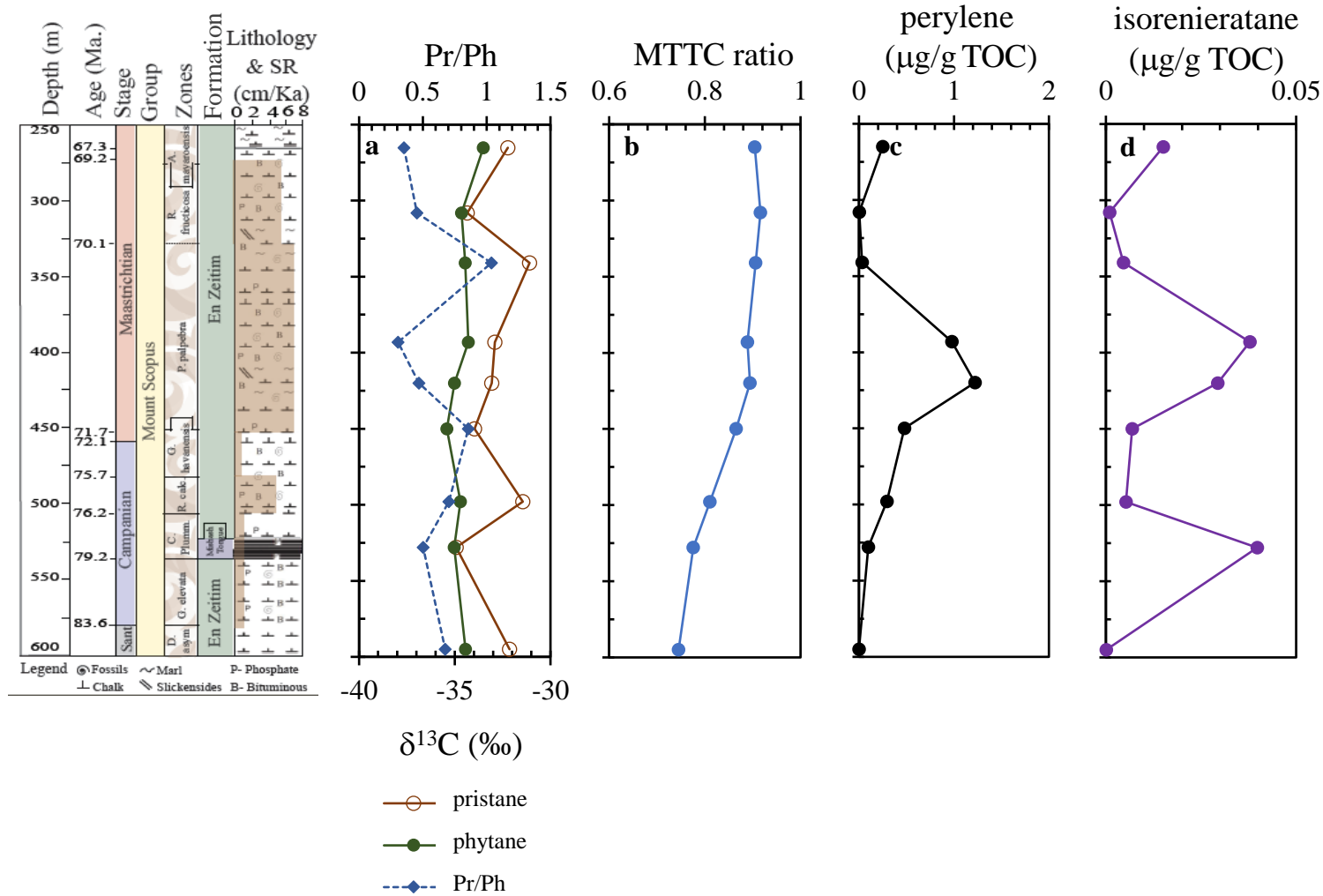


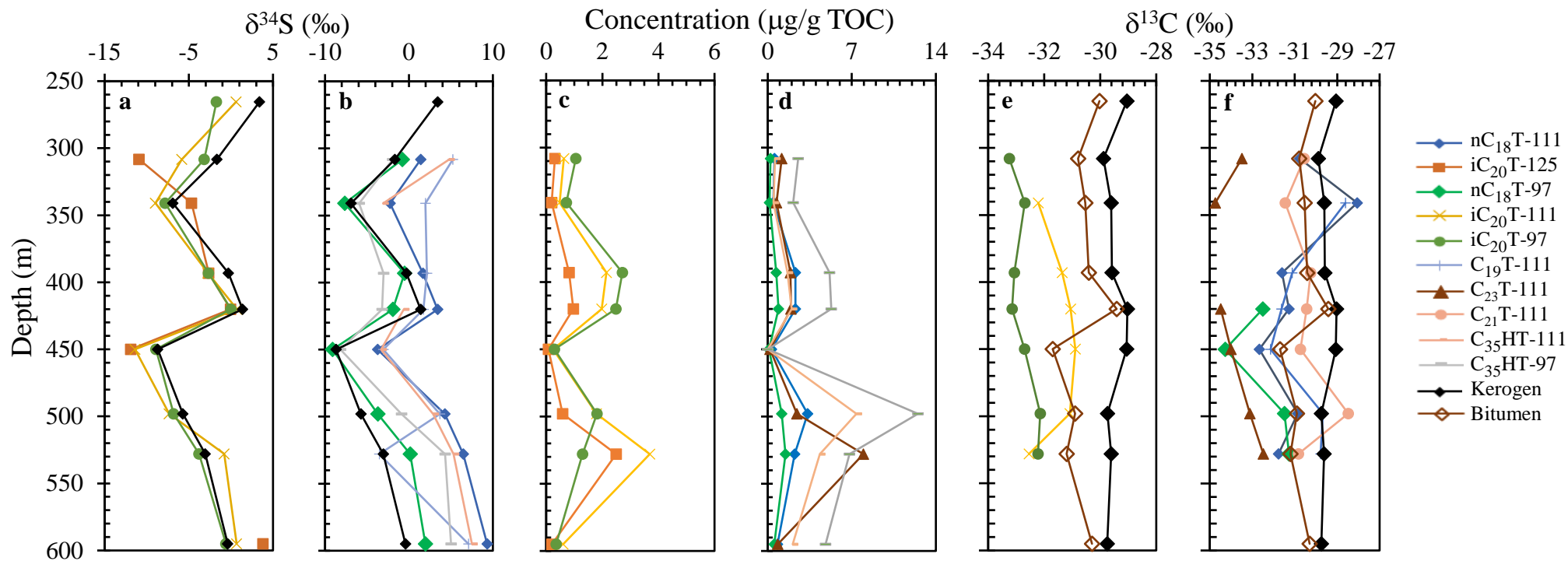
Fig.2

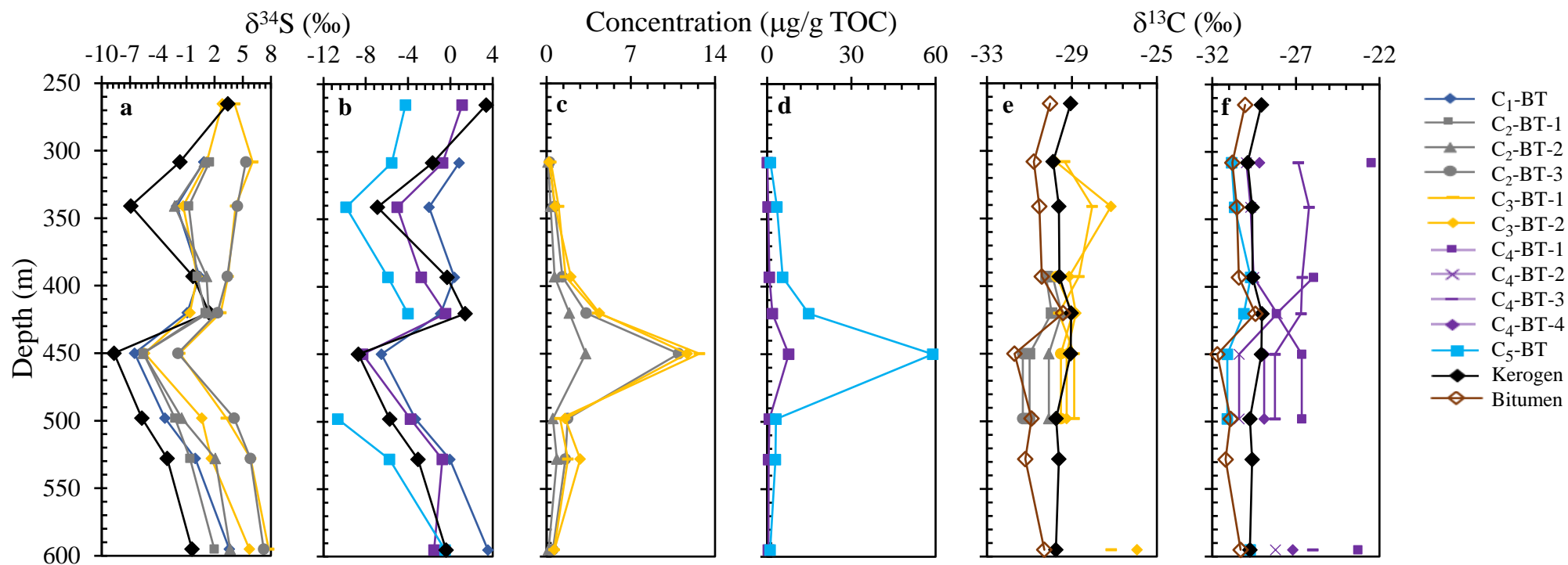
Fig.3

Fig.4

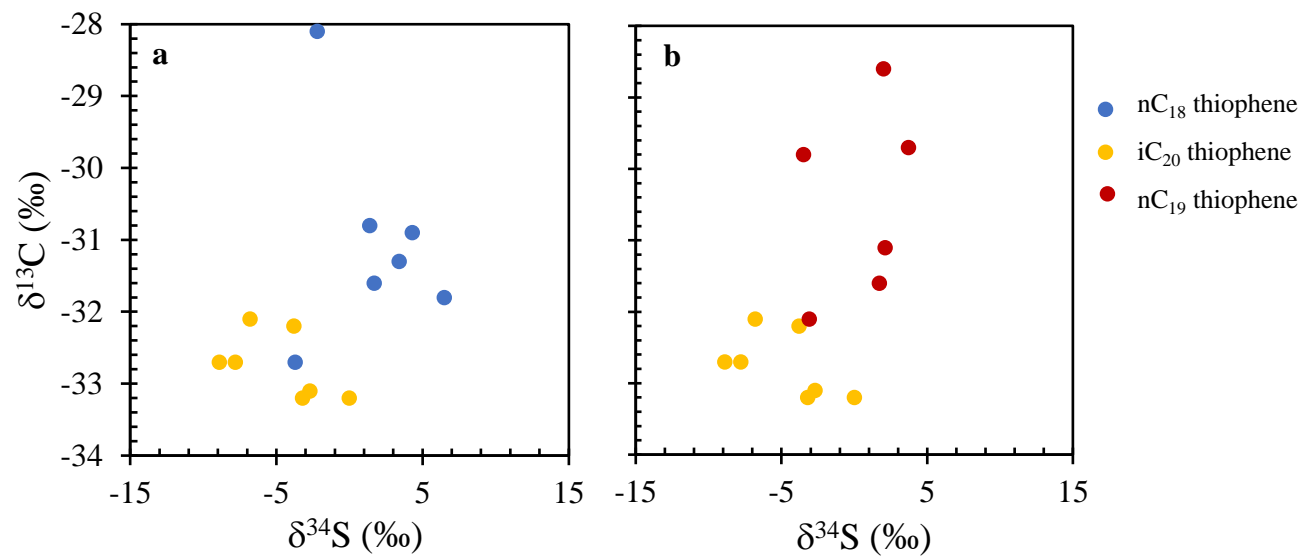


Fig.5

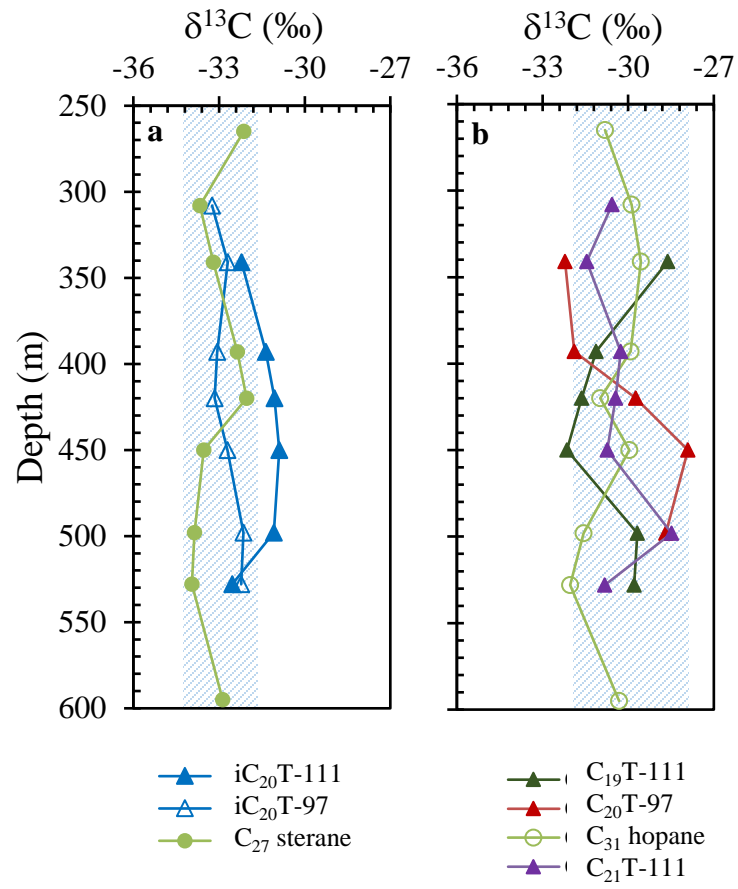


Fig.6

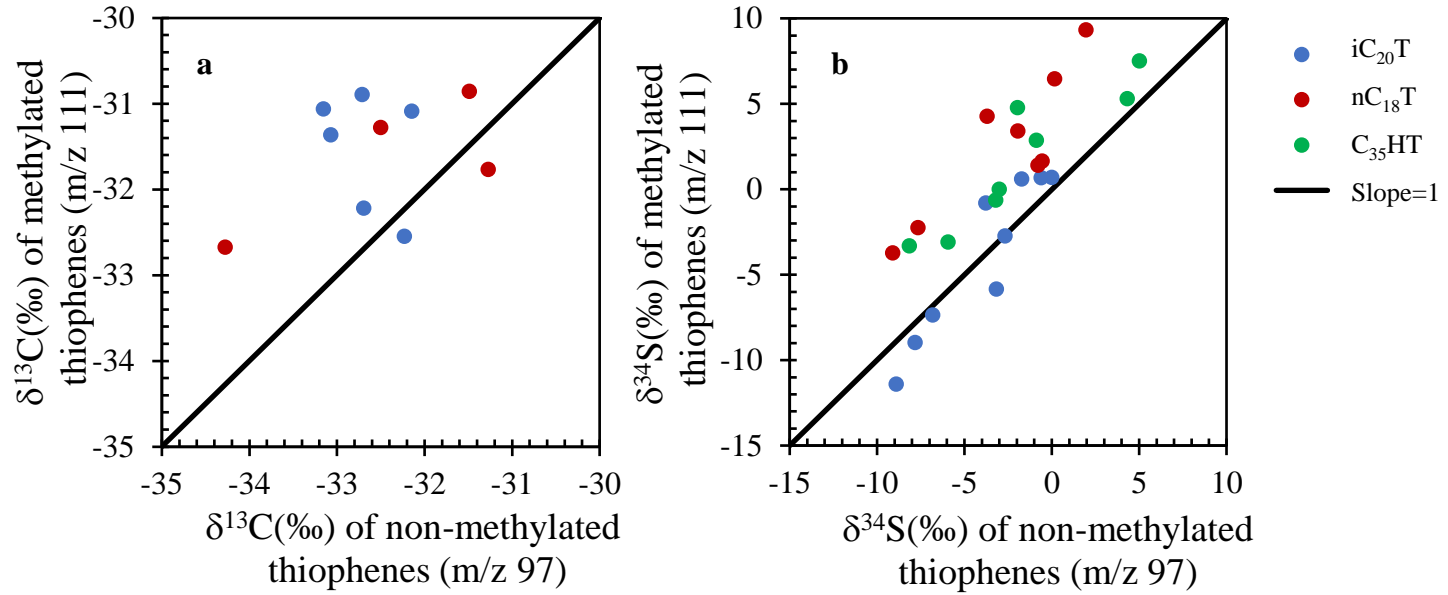


Fig.7

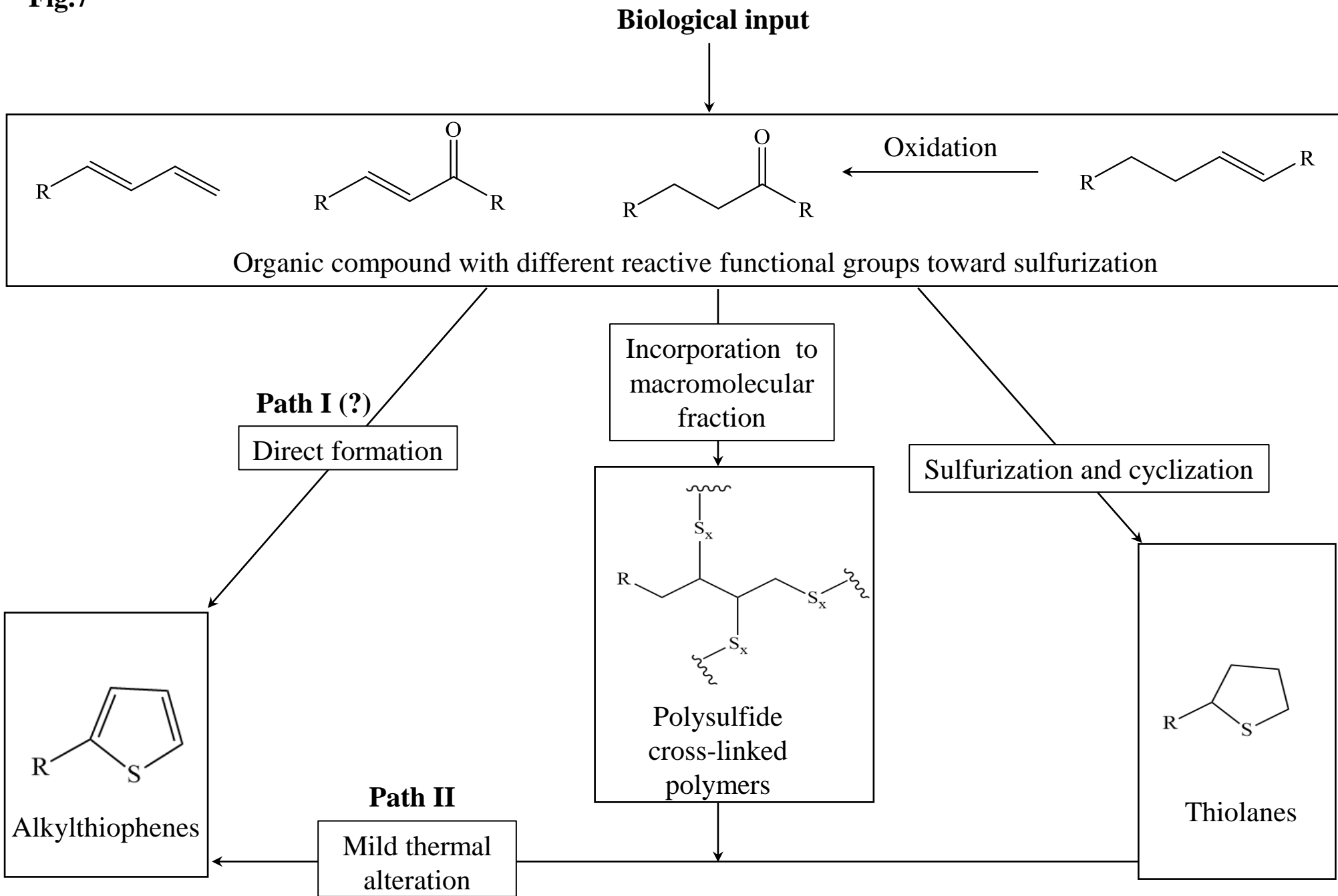


Fig.8

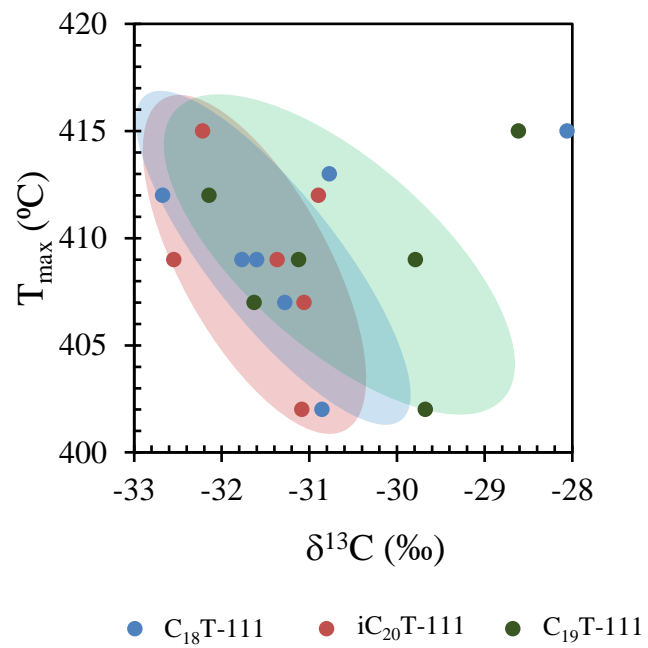


Fig.9

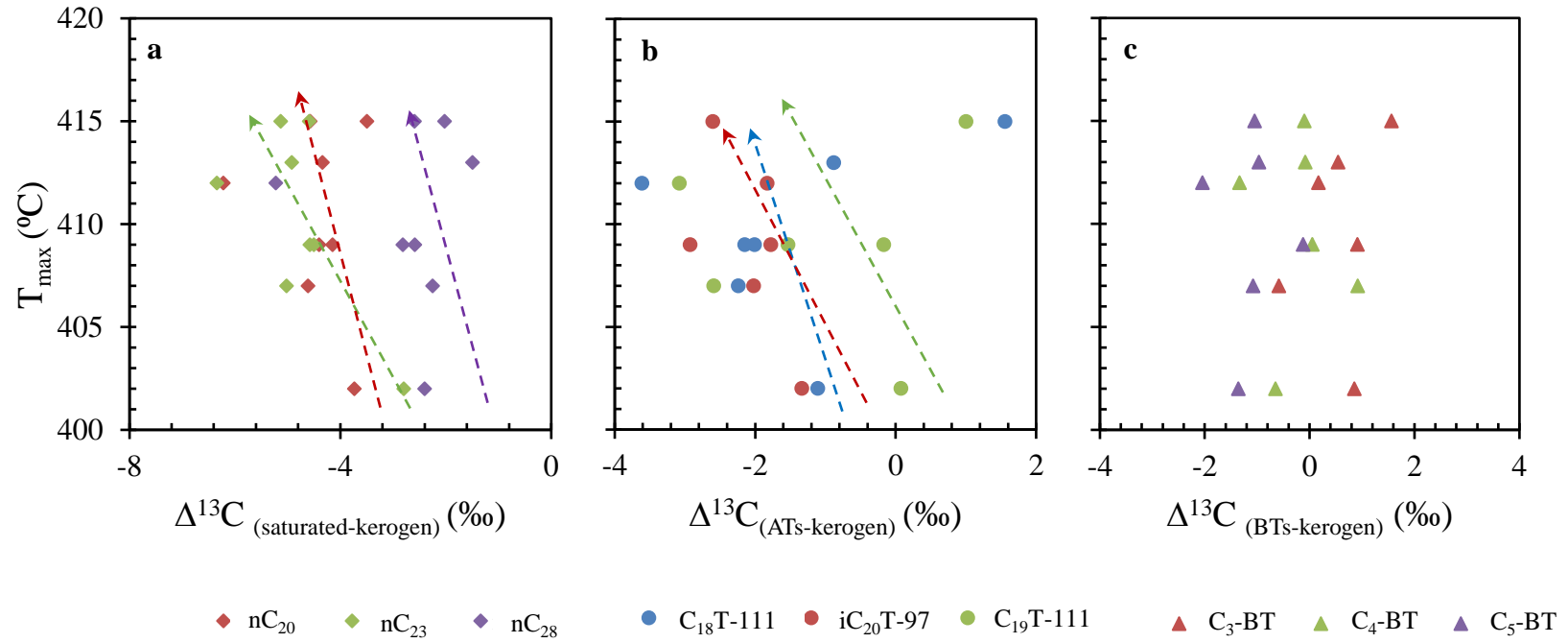


Fig.10

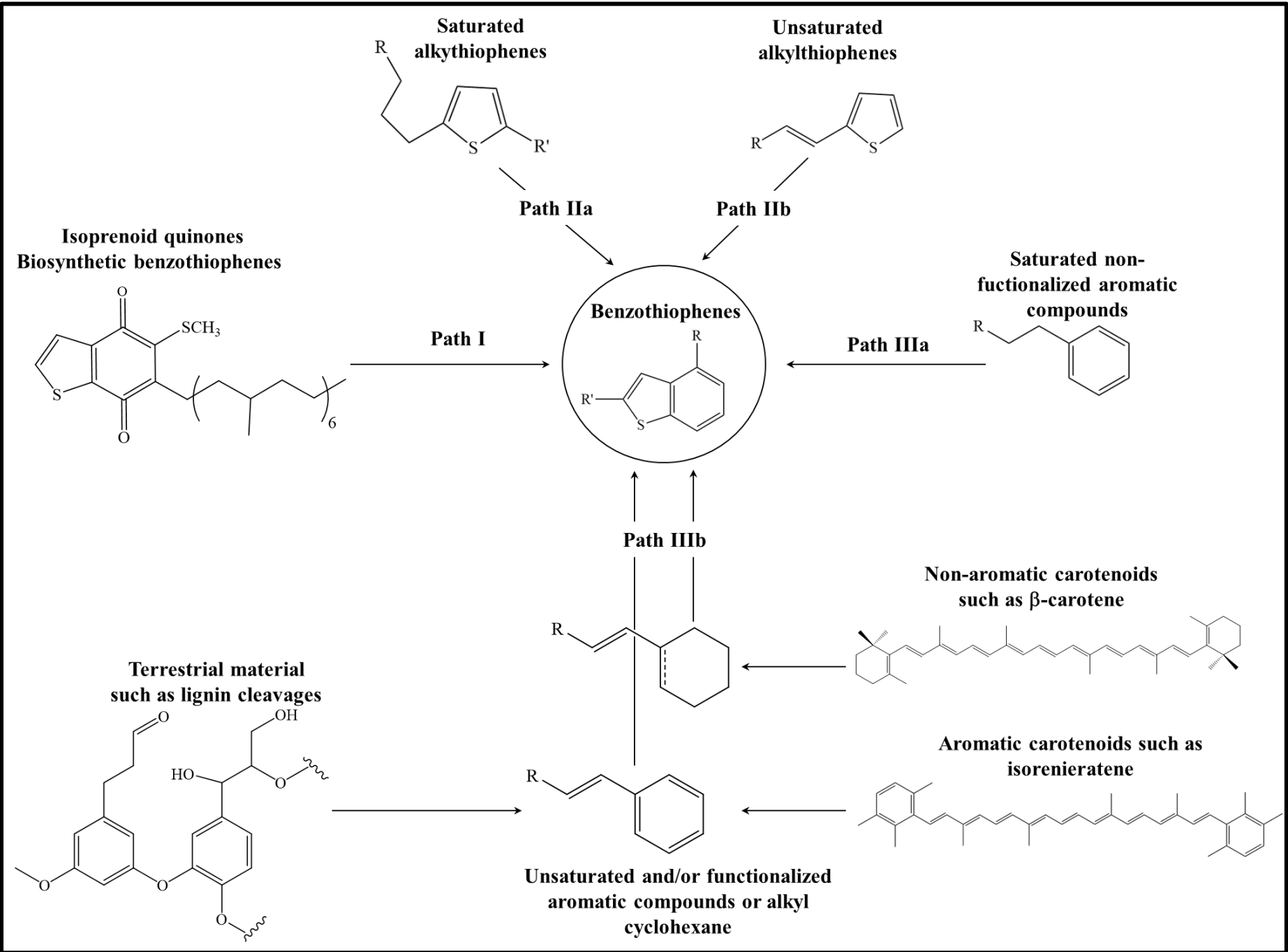


Table 1: The $\delta^{13}\text{C}$ values (‰) of normal alkanes, isoprenoids, hopanes and steranes of the saturated fraction extracted from the Ghareb Formation samples.

Compound name	Depth (m)								
	265	308	341	393	420	450	498	528	595
Normal alkanes									
^a nC ₁₃	-	-	-	-34.3±0.1	-34.7±0.1	-	-	-	-
nC ₁₄	-	-30.0±0.1	-	-33.7±0.1	-34.1±0.1	-34.8±0.1	-32.3±0.2	-30.9±0.0	-
nC ₁₅	-30.1±0.1	-34.8±0.1	-35.1±0.1	-34.2±0.1	-34.5±0.1	-36.3±0.0	-32.8±0.0	-34.8±0.1	-32.4±0.2
nC ₁₆	-32.5±0.1	-34.1±0.1	-34.4±0.1	-33.8±0.0	-34.5±0.1	-36.2±0.1	-33.4±0.1	-34.5±0.2	-32.1±0.2
nC ₁₇	-33.2±0.2	-34.4±0.1	-34.9±0.2	-34.5±0.1	-35.1±0.1	-36.6±0.1	-33.8±0.1	-35.2±0.0	-32.5±0.1
nC ₁₈	-32.5±0.2	-34.4±0.1	-34.6±0.0	-33.7±0.0	-34.4±0.1	-35.9±0.1	-34.3±0.0	-34.6±0.1	-32.6±0.1
nC ₁₉	-32.9±0.3	-34.5±0.1	-34.2±0.2	-34.0±0.1	-34.2±0.1	-35.7±0.1	-33±0.2	-34.1±0.1	-32.4±0.0
nC ₂₀	-32.6±0.1	-34.2±0.1	-34.2±0.0	-33.7±0.2	-33.6±0.0	-35.3±0.1	-33.5±0.1	-34.0±0.0	-32.9±0.2
nC ₂₁	-33.6±0.1	-35.2±0.1	-34.8±0.2	-34.5±0.2	-34.1±0.1	-35.7±0.1	-33.9±0.2	-34.1±0.1	-32.2±0.0
nC ₂₂	-32.9±0.2	-34.7±0.1	-34.1±0.1	-34.4±0.0	-33.8±0.1	-35.3±0.1	-33.2±0.1	-34.3±0.1	-31.8±0.1
nC ₂₃	-33.6±0.1	-34.8±0.1	-34.7±0.0	-34.2±0.0	-34.1±0.0	-35.4±0.0	-32.5±0.1	-34.1±0.1	-31.9±0.0
nC ₂₄	-32.4±0.1	-34.0±0.1	-33.8±0.2	-33.8±0.1	-33.7±0.1	-35.5±0.0	-32.7±0.1	-33.5±0.1	-31.4±0.1
nC ₂₅	-32.1±0.1	-32.6±0.1	-32.6±0.2	-32.0±0.1	-32.3±0.0	-34.0±0.1	-31.1±0.1	-	-31.5±0.1
nC ₂₆	-31.8±0.1	-32.0±0.1	-31.9±0.1	-32.2±0.0	-32.9±0.1	-34.9±0.1	-31.9±0.2	-31.9±0.1	-30.4±0.1
nC ₂₇	-32.4±0.2	-32.3±0.1	-32.4±0.1	-31.8±0.1	-32.7±0.1	-34.5±0.1	-31.8±0.0	-32±0.1	-30.8±0.0
nC ₂₈	-31.7±0.2	-31.4±0.2	-31.6±0.1	-32.4±0.1	-31.3±0.3	-34.3±0.1	-32.1±0.0	-32.2±0.1	-31.2±0.3
nC ₂₉	-31.8±0.2	-32.4±0.2	-32.5±0.1	-33.1±0.1	-32.1±0.0	-34.1±0.1	-31.2±0.1	-30.6±0.2	-30.3±0.1
Isoprenoids									
pristane	-32.2±0.2	-34.3±0.2	-31.1±0.1	-32.9±0.2	-33.1±0.1	-34.0±0.2	-31.4±0.1	-34.9±0.1	-32.1±0.1
phytane	-33.5±0.1	-34.6±0.1	-34.4±0.0	-34.3±0.0	-35.0±0.1	-35.4±0.1	-34.7±0.1	-35.0±0.1	-34.4±0.1
Hopanes									
17 α - trishnorhopane	-31.1±0.2	-	-	-	-	-	-30.9±0.1	-	-28.8±0.1
17 α -norhopane	-30.0±0.2	-	-	-	-	-	-30.4±0.2	-	-30.1±0.0
^b C ₃₁ hopane-1	-30.8±0.4	-29.9±0.1	-29.6±0.2	-29.9±0.3	-31.0±0.3	-30.0±0.2	-31.6±0.2	-32.0±0.3	-30.3±0.1
C ₃₁ hopane-2	-28.6±0.3	-28.4±0.2	-28.2±0.2	-27.8±0.1	-27.9±0.3	-27.5±0.1	-28.9±0.1	-	-27.8±0.2
C ₃₁ hopane-3	-	-	-	-	-	-	-	-	-30.7±0.1
Steranes									
C ₂₇ sterane-1	-32.2±0.2	-33.2±0.1	-32.6±0.2	-31.8±0.2	-31.8±0.2	-33.4±0.2	-32.3±0.1	-33.6±0.2	-31.1±0.1
C ₂₇ sterane-2	-32.1±0.1	-33.7±0.2	-33.2±0.1	-32.4±0.2	-32.0±0.2	-33.5±0.1	-33.9±0.1	-34.0±0.1	-32.9±0.2
C ₂₈ sterane-1	-31.1±0.3	-	-	-	-	-	-	-	-
C ₂₈ sterane-2	-32.4±0.2	-33.9±0.2	-33.9±0.3	-33.2±0.2	-30.5±0.3	-34.6±0.1	-27.2±0.1	-32.3±0.1	-
C ₂₉ sterane	-29.7±0.1	-31.8±0.2	-32.8±0.2	-32.1±0.1	-32.7±0.3	-33.7±0.1	-	-	-

^an= normal.^bT_m stands for C₂₇ 17 α - hopane.^cThe numbers in hopanes and steranes names represent different isomers.



Click here to access/download

Supplementary Material

Sahwar_13C_34S_Supplementary.docx

